Available online at www.sciencedirect.com
ScienceDirect
Journal of Sound and Vibration 300 (2007) 612–643
JOURNAL OF SOUND AND VIBRATION
www.elsevier.com/locate/jsvi

Vibration suppression of structures with densely spaced modes using maximally robust minimum delay digital finite impulse response filters

G.N. Glossiotis, I.A. Antoniadis*

Department of Mechanical Engineering, Mechanical Design and Control Systems Division, National Technical University of Athens, 9 Heroon Polytechniou Street, 15773 Athens, Greece

Received 30 August 2005; received in revised form 21 July 2006; accepted 25 July 2006
Available online 31 October 2006

Abstract

Due to the inherent flexibility of engineering structures, transient and residual vibrations occur when a motion command is applied, thus raising several practical restrictions concerning their fast, accurate and safe motion. Although various command-preconditioning techniques have been proposed for the effective suppression of the excited vibrations, their application has been limited only to structures with a few distinct and well-separated modes. This paper further considers the applicability of motion preconditioning methods for a large class of lightweight flexible structures, which present multiple densely spaced natural modes, existing even at relatively low frequencies. Properly designed finite impulse response (FIR) filters can lead to an effective motion preconditioning method, suppressing drastically the excited vibrations over the entire excited frequency band. Compared to other alternative preconditioning methods, such as input shapers or infinite impulse response (IIR) filters, FIR filters present the most efficient behavior in terms of vibration suppression efficiency, or in terms of the delay introduced in the motion command, as verified by numerical simulations and experimental results involving multibay trusses, with tenths of densely spaced modes in a range from 0.4 Hz up to 75 Hz.

1. Introduction

Due to the inherent flexibility of engineering structures, transient and residual vibrations occur when a motion command is applied, thus raising several practical restrictions concerning their fast, accurate and safe motion. The traditional approaches to minimize the effect of this type of vibrations are focused on either passive vibration methods, which necessitate modifications of the structure and thus frequently result in an increase of the size and the weight of the structure, or on closed loop control methods, namely active vibration suppression methods, which require advanced instrumentation and control equipment and thus may result in an increased complexity and failure liability of the structure.

*Corresponding author. Tel.: +30 1 772 1524; fax: +30 1 772 1525.
E-mail address: antogian@central.ntua.gr (I.A. Antoniadis).

0022-460X/$ - see front matter © 2006 Elsevier Ltd. All rights reserved.
doi:10.1016/j.jsv.2006.07.049

An alternative approach for suppressing vibrations generated by a motion command is the proper conditioning of the prespecified motion pattern (which is called ''Command'' or ''Control Input'' or, simply, ''Input''), so that the system moves to the desired position with the minimum level of vibrations. The basic advantage of command preconditioning methods over the traditional passive or active vibration suppression methods is their quite simple implementation, since they require just a proper modification of the original motion profile. Parallel, preconditioning methods can be either used individually as stand alone motion control schemes or supplement the afore-mentioned traditional methods.

The first approach of command preconditioning, proposed by Smith [1], used a partitioning of the desired excitation pattern into two distinct steps, the second one of which is delayed. Since then, substantial research effort has been devoted towards the development of preconditioning techniques, focusing especially to the optimal compromise between the speed of the response, the robustness (or insensitivity) with respect to variations of dynamic parameters of the system and the level of residual vibrations.

Among preconditioning methods, ''Input Shapers'' are the most commonly used class that has drawn special attention due to their ease of implementation, since they can be applied to convolve any arbitrary input to a system with a series of impulses. Singer and Seering [2] introduced input shaping theory for the motion of single-degree-of-freedom LTI systems and provided a method to increase the robustness characteristics at each single mode. Singhose et al. [3] proposed the multihump class of input shapers in order to further improve the robustness characteristics over a single mode, while Shan et al. [4] further extended the above design procedures by proposing the modified input shaping (MIS).

In the case of systems with multiple modes, Singer and Seering [2] proposed the concept for the design of input shapers for systems with multiple modes, either by further convolving the basic impulse pattern for every distinct mode, or by solving the constraint equations for all modes simultaneously. Singh and Vadali [5,6], Tuttle and Seering [7] and Park et al. [8] described different approaches for the design of input shapers in the discrete domain, by appropriately placing zeros at the poles of the flexible system on the z-plane. Pao and Cutforth [9] proposed a method for the design of input shapers in the frequency domain with increased robustness characteristics.

Concerning the actual application and validation of input shaping methods for systems with multiple degrees of freedom, Hyde [10,11] performed numerical experiments to dynamic models of flexible space structures with up to four distinct modes, applying methods proposed in Ref. [2]. Rappole [12] and Chang [13] applied the same methods [2] in real time experiments, using flexible structures with four and five distinct modes, respectively. Tuttle and Seering [7] verified experimentally their proposed method to the test bed of a space structure, by successfully applying a four mode input shaper. Doherty and Tolson [14] applied numerically the same technique to the model of a space satellite, using an eight-mode input shaper.

Since the initially proposed forms of input shapers [2] can be considered as specific cases of digital notch finite impulse response (FIR) filters [15], Economou et al. [16–18] considered the application of conventional digital filters for motion command preconditioning as an alternative for input shapers. After a systematic consideration of several types of conventional FIR filters, it has been demonstrated that three types of them can present substantially increased robustness to variations of the system natural frequencies, while simultaneously introducing the minimum possible delay and vibration error [16]. The research was extended to four types of conventional infinite impulse response (IIR) filters [17], showing that although in general FIR filters present a better behavior in terms of robustness and time delay, IIR filters may offer a number of advantages, such as reduction of computational effort, which might be crucial in real-time applications, as well as a better overall vibration suppression quality. However, the actual application and validation of the method by Economou et al. has been limited to an experimental study of a rotating beam with a variable mass attached at its end [16,17], were only the first mode was practically excited, without any systematic comparisons to other alternative preconditioning methods.

In this paper, the application of motion preconditioning methods are further considered to structures, where multiple and densely packed modes are simultaneously excited by the motion commands. Lightweight flexible structures of this type are often encountered in a number of engineering applications, in most cases incorporated as essential components in larger mechanical systems, which as a direct result influence even more their dynamic response in a rather complex manner. This is because such structures generally possess high modal densities, with clusters of densely packed modes, existing even at relatively low frequencies [19–22].

Due to the fact that the robustness of the existing input shaping methods is restricted in narrow bands around the system natural frequencies, which among others further reduces their efficiency by the accuracy of the modal identification of the system [14], the application of input shapers has been limited to flexible structures with a few modes, where the natural frequencies were quite distinct and well separated in the frequency domain. Thus, no systematic application of motion preconditioning techniques has been attempted to structures with multiple densely spaced modes, since almost all the applications of motion preconditioning techniques to structures with multiple modes have been based on various forms of input shapers.

In this paper it is shown, that efficient motion preconditioning can be also achieved for structures with multiple and densely spaced modes, based on conventional FIR filters. Since properly designed FIR filters can present a significantly wider stop-band than input shapers, while simultaneously introduce less motion delay than conventional IIR filters, they present currently the best approach to handle applications with this modal structure.

A summary of the necessary theoretical framework for the application of digital filters for motion command preconditioning is presented in Section 2 and the design concepts and the advantages offered by properly designed FIR filters is presented in Section 3. A multibay truss is considered is Section 4, with more than 50 densely packed modes, covering almost entirely a frequency band between 1 and 70 Hz. Three different preconditioning approaches by FIR filters, by IIR filters and by Input Shaping are compared, using extended numerical simulations. A relevant experimental application is presented in Section 5, involving a multibay truss with more than 20 densely spaced modes in a range from 0.4 to 75 Hz.

2. Revision of basic concepts of input preconditioning

2.1. Requirements for vibration suppression using input preconditioning

As has been shown among others in Ref. [17], the state space response of the principal (natural or normal) coordinates or modes $\mathbf{p}_i(t)$ of a linear multidegree of freedom (MDOF) system can be written by the following set of independent (uncoupled) equations:

$$\mathbf{p}_i(t) = \mathrm{e}^{\mathbf{A}_i t}\mathbf{p}_i(0) + \int_o^t \mathrm{e}^{\mathbf{A}_i(t-\tau)}\mathbf{b}g_i(\tau)\,\mathrm{d}\tau = \mathrm{e}^{\mathbf{A}_i t}\left[\mathbf{p}_i(0) + \int_o^t \mathrm{e}^{-\mathbf{A}_i\tau}\mathbf{b}g_i(\tau)\,\mathrm{d}\tau\right], \quad i = 1,\ldots,L \tag{1}$$

or equivalently by

$$\mathbf{p}_i(t) = \mathrm{e}^{\mathbf{A}_i t}\left[\mathbf{p}_i(0) + \sum_{j=1}^{2} H_{i,j}\mathbf{b}\int_o^t \mathrm{e}^{-\lambda_i\tau}g_i(\tau)\,\mathrm{d}\tau\right] \tag{2a}$$

$$= \mathrm{e}^{\mathbf{A}_i t}\left[\mathbf{p}_i(0) + \sum_{j=1}^{2} H_{i,j}\mathbf{b}G_i(s; s=\lambda_{i,j})\right], \quad i = 1,\ldots,L, \tag{2b}$$

where L is the number of degrees of freedom, $g_i(t)$ are the corresponding generalized forces with a corresponding Laplace transform $G_i(s)$, ω_i are the natural frequencies of the system with corresponding damping ratios ζ_i and eigenvectors $\mathbf{V}_i$, $\mathbf{x}(t)$ is the vector of external forces and

$$\mathbf{A}_i = \begin{bmatrix} 0 & 1 \\ -\omega_i^2 & -2\zeta_i\omega_i \end{bmatrix}, \quad \mathbf{b} = \begin{bmatrix} 0 \\ 1 \end{bmatrix}, \quad i = 1,\ldots,L, \tag{3a}$$

$$g_i(t) = \mathbf{V}_i^{\mathrm{T}}\mathbf{x}(t) = \sum_{m=1}^{L} V_{i,m}x_m(t), \tag{3b}$$

$$\mathbf{V}_i^{\mathrm{T}} = [V_{i,1}, V_{i,2}, \ldots, V_{i,L}], \tag{3c}$$

$$\mathbf{x}^{\mathrm{T}}(t) = [x_1(t), x_2(t), \ldots, x_L(t)], \tag{3d}$$

$$e^{\mathbf{A}_i t} = \sum_{j=1}^{2} e^{\lambda_{i,j} t} \mathbf{H}_{i,j}, \tag{3e}$$

$$\lambda_{i,1-2} = -\zeta_i \omega_i \pm \omega_i \sqrt{1-\zeta_i^2}, \tag{3f}$$

$$\mathbf{H}_{i,j} = \frac{1}{\lambda_{i,j} - \lambda_{i,k}} [\mathbf{A}_i - \lambda_{i,j} \mathbf{I}] \quad \text{for } j,k = 1,2 \ j \neq k. \tag{3g}$$

In the case that the principal coordinate corresponds to a "rigid body" mode of the system, the corresponding natural frequency ω_i of the system is zero and Eq. (2b) can be similarly shown to take the specific form:

$$\mathbf{p}_r(t) = \mathbf{H}_r(t)\big[\mathbf{p}_r(0) + \mathbf{b} G_r(s; s=0)\big], \quad r = 1, \ldots, L_r, \tag{4a}$$

$$\mathbf{H}_r(t) = \begin{bmatrix} 1 & t \\ 0 & 1 \end{bmatrix}, \tag{4b}$$

where L_r denotes the number of the "rigid body" modes of the system.

In view of Eq. (2b), the requirement for vibration suppression can be stated as

$$G_i(s; s = \lambda_{i,j}) = 0. \tag{5}$$

Thus, the basic concept of all preconditioning methods is that instead of the original generalized input forces $g_i(t)$, conditioned generalized input forces $q_i(t)$ can be used, obtained by the original ones $g_i(t)$, (or equivalently by the original input vector $\mathbf{x}(t)$) by

$$Q_i(s) = F(s) G_i(s) = \sum_{m=1}^{L} V_{i,m} [F(s) X_m(s)] = \sum_{m=1}^{L} V_{i,m} Y_m(s), \quad i = 1, \ldots, L, \tag{6a}$$

$$q_i(t) = \mathbf{V}_i^{\mathrm{T}} \mathbf{y}(t) = \sum_{m=1}^{L} V_{i,m} y_m(t), \tag{6b}$$

$$Y_i(s) = F(s) X_i(s), \tag{6c}$$

where $X_m(s)$ and $Y_m(s)$ denote the Laplace transforms of $x_m(t)$ and $y_m(t)$, respectively.

In this case, the corresponding Laplace transform $Q_i(s)$ of $q_i(t)$ appears in Eqs. (2b), (4a) and (5) instead of $G_i(s)$.

The purpose of introducing Eq. (6), is that the conditioned generalized forces $q_i(t)$ are able to move the system in essentially the same way as the original input functions $g_i(t)$, without the effect of the residual vibrations. Taking into account Eqs. (2b), (5) and (6a), this requirement can be written as

$$Q_i(s; s = \lambda_{i,j}) = 0 \Leftrightarrow F(s; s = \lambda_{i,j}) = 0, \tag{7a}$$

$$Q_i(s; s = 0) = G_i(s; s = 0) \Leftrightarrow F(s; s = 0) = 1. \tag{7b}$$

In view of Eqs. (2b) and (5), Eq. (7a) implies that the residual vibration effect can be completely canceled just by the proper selection of the preconditioning function $F(s)$, quite independently from the properties of the original input function $g_i(t)$. On the other hand, in view of Eq. (4a), Eq. (7b) implies that $q_i(t)$ maintains all the properties that $g_i(t)$ posses, in order to move the system as a rigid body.

Furthermore, Eq. (6) clearly imply that since the conditioning approach affects only the excitation function of the system, its dynamic properties, as expressed by the natural frequencies ω_i and the damping ratios ζ_i, remain unmodified.

2.2. Realization of the preconditioning function using digital filters

Among others, the realization of the preconditioning function $F(s)$ can be achieved by a convolution procedure, resulting in a discrete filtered signal $q_i(kT_S)$, which is obtained from an original discrete input signal $g_i(kT_S)$ using a recursive sequence of the form:

$$q_i(t) = \sum_{n=0}^{N} c_n g_i(t - nT_S) - \sum_{n=1}^{M} a_n q_i(t - nT_S), \quad i = 1, \ldots, L \tag{8a}$$

or equivalently

$$y_i(t) = \sum_{n=0}^{N} c_n x_i(t - nT_S) - \sum_{n=1}^{M} a_n y_i(t - nT_S), \quad i = 1, \ldots, L, \tag{8b}$$

where k is an integer, T_S is the sampling period of the discrete signals $q_i(t_n)$ and $g_i(t_n)$ (filter sampling period) and $\{c_n\}$ and $\{a_n\}$ are series of constants (filter coefficients) of length $N+1$ and M, respectively.

In the case of FIR filters, all coefficients of the $\{a_n\}$ series are equal to zero. Otherwise, the filter is of IIR type. Input shapers are actually specific forms of FIR filters, where the coefficients $\{c_n\}$ are selected according to the various methods proposed for the design of input shapers.

In this case, the corresponding Laplace transform $F(s)$ of the preconditioning function is written as

$$F(s) = \frac{\sum_{n=0}^{N} c_n \mathrm{e}^{-snT_S}}{1 + \sum_{n=1}^{M} a_n \mathrm{e}^{-snT_S}} \tag{9a}$$

with a corresponding z-transform:

$$F(z) = \frac{\sum_{n=0}^{N} c_n z^{-n}}{1 + \sum_{n=1}^{M} a_n z^{-n}} \tag{9b}$$

and corresponding Frequency Response Function (FRF):

$$F(\mathrm{j}\omega) = F(\mathrm{j}2\pi f) = \frac{\sum_{n=0}^{N} c_n \mathrm{e}^{-\mathrm{j}n2\pi f T_S}}{1 + \sum_{n=1}^{M} a_n \mathrm{e}^{-\mathrm{j}n2\pi f T_S}}, \quad f \text{ in Hz.} \tag{9c}$$

Eq. (7) clearly imply that the design of a proper function $F(s)$, is completely equivalent to the design of a filter in the form of Eq. (9).

3. Filter design concepts and properties

3.1. The low-pass filter concept for robust residual vibration suppression

Provided that the FRF $F(\mathrm{j}\omega)$ of Eq. (9c) of the filter is zero at frequencies coinciding with the expected natural frequencies of the dynamic system according to Eq. (7a), this filter is capable of completely eliminating the residual vibrations effect. Considering further the requirement for robust residual vibration suppression, the robustness properties for the preconditioning procedure can be directly met, by extending the requirement for zero frequency response of the filter not only for individual frequencies coinciding with the expected natural frequencies of the system, but also for extended areas (stop-band areas) of the filter FRF $F(\mathrm{j}\omega)$, in order to cover now additionally the possible variations of the system natural frequencies. In addition, according to Eq. (7b), the response for zero frequency of this filter should be kept equal to one, in order to ensure the proper motion of the mechanical system as a rigid body.

Thus, an ideal filter must have a low-frequency band with a frequency response equal to one and a high-frequency range with a frequency response equal to zero for frequencies equal to or higher than the natural frequencies of the flexible system. This type of frequency response can be achieved by a low-pass filter.

3.2. Filter design requirements and performance indices

However, due to inherent design constraints [16], the low-pass filters that can be realized in practice, present a frequency response that differs from the ideal one. Fig. 1 presents the ideal and the actual response function of a typical low-pass digital filter.

Low-pass filters have a pass-band upper limited by the filter pass-band frequency f_B and a stop-band lower limited by the filter cut-off frequency f_C. The frequency range of the stop-band is defined by the stop band width w_{SB}:

$$w_{SB} = f_{SF} - 2f_C, \tag{10}$$

where $f_{SF} = 1/T_S$ is the sampling frequency of the filter.

Thus, in an actual low-pass filter, a transition band (response between 1 and 0) exists between the pass-band and the stop-band and, also, its frequency response presents ripples in the pass-band and the stop-band (deviations from the ideal values of one and zero, respectively). Since the ripples in the stop-band prevent Eq. (7a) to be exactly satisfied, a small amount of vibration must be accepted:

$$e_S \leqslant (e_S)_{per} \Leftrightarrow F(s, s = \lambda_{i,j}) \leqslant (e_S)_{per}, \tag{11}$$

where $(e_S)_{per}$ is the acceptable size of the ripples in the stop-band, which also represents the maximum permissible vibration error.

Furthermore, the filtering process introduces a delay T_D in the application of the commanded input to the system, which is equal to the total time duration of the filter in the case of linear phase symmetric FIR filters.

Thus a filter, capable of robustly suppressing residual vibrations, must satisfy the following requirements:

(R.a) Cut-off frequency f_C lower than or equal to the system's expected smallest natural frequency f_0.
(R.b) Stop-band width w_{SB} quite large, in order to ensure the robust behavior of the filter in case that the natural frequencies are inaccurately predicted or varying, as well as to cover the system's higher natural frequencies.
(R.c) Response for zero frequency equal to one, in order to achieve appropriate rigid body motion as required by Eq. (7b).

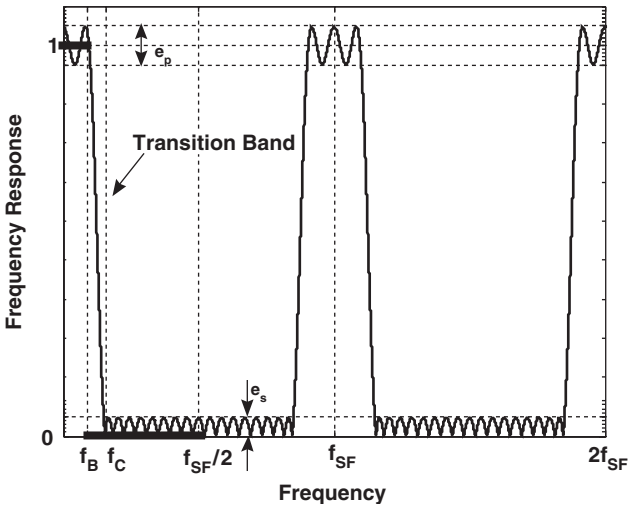

Fig. 1. Typical frequency response of an ideal and a real low-pass filter. ▬▬, ideal filter; ———, real filter.

(R.d) Ripples on the stop-band smaller than a prespecified acceptable residual vibration error as required by Eq. (11).
(R.e) Minimum possible filter delay T_D.

It should be mentioned that the requirement (R.d) for the simultaneous minimization of the residual vibration error, the requirement (R.e) for the minimization of the filter delay and the requirement (R.b) for the maximization of the filter robustness are contradicting to each other.

Therefore, in order to measure the degree to which a specific filter meets the above requirements, a set of filter performance indices is defined:

(a) The relative robustness r_R to variations of the system natural frequencies:

$$r_R = \frac{w_{SB}}{f_0} = \frac{f_{SF} - 2f_C}{f_0} = \frac{f_{SF} - 2f_C}{f_C} \tag{12}$$

assuming that the cut-off frequency f_C is selected equal to the lowest natural frequency f_0 of the system.

(b) The relative robustness width r_W covered by the robustness region (stop-band) of the filter in proportion to the overall effective frequency range of the filter:

$$r_W = \frac{w_{SB}}{f_{SF}} = \frac{f_{SF} - 2f_C}{f_{SF}}. \tag{13}$$

(c) The relative delay d introduced by the filter:

$$d = \frac{T_D}{T_0} = f_0 T_D, \tag{14}$$

where T_0 the highest natural period of the system.

3.3. Advantages of maximally robust time-optimal parametric FIR filters

A general design procedure has been proposed in Ref. [16], leading to a selection of the parameters of any FIR filter type, which optimally fulfills the requirements of Section 3.2. Using this procedure, a library of conventional FIR filters has been parametrically predesigned, able to be readily applied to any specific dynamic system, according to the procedures described in Ref. [16]. Among the several classes of conventional filters tested, three classes of conventional FIR filters present the best behavior:

(A) the Parks–McClellan filter type;
(B) the Chebyshev window-based filter type;
(C) the constrained least-squares-based filter type.

Examples of the FRF of such filters are shown in Fig. 2. Three different filters of the Parks–McClellan type are presented, with orders of $N = 4$, $N = 16$ and $N = 64$, respectively.

Comparing the FIR filters resulting from the design procedure in Ref. [16] to the various forms of input shapers, it should be noted that for applications in single degree of freedom systems, the resulting FIR filters coincide to certain classes of input shapers. For example, the Parks–McClellan filter of order $N = 4$ in Fig. 2a coincides to the extra insensitive input shaper designed for an undamped mode, as proposed in Ref. [3].

However, the basic advantage of the FIR filters designed as in Ref. [16] over the various forms of input shapers, is the concept by which both methods approach structures with multiple natural frequencies. Input shapers are in principle designed to cover robustness requirements around one specific natural frequency, using several alternative procedures [2,3]. In order to be applied to systems with multiple modes, the most general and effective input shaping procedure consists in designing first a number of different specific single mode input shapers for the suppression of each one natural frequency of the system and then convolving in the time domain all the resulting single mode input shapers, leading thus to a unique impulse sequence in the time

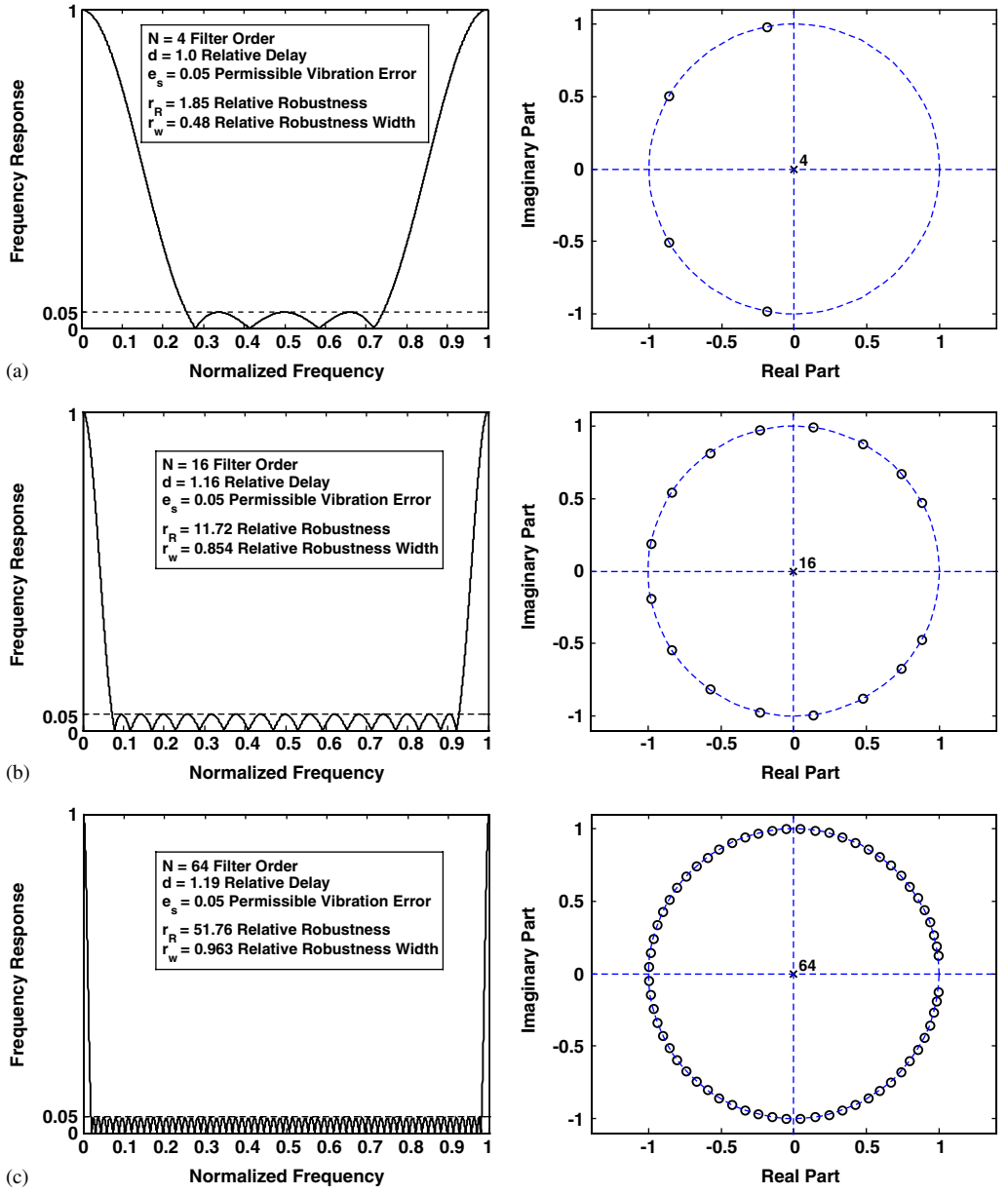

Fig. 2. Frequency response of FIR filters of Parks–McClellan type, and their corresponding zero-pole plots with reference to the unit circle (z-plane), for three different filter orders: (a) $N = 4$, (b) $N = 16$ and (c) $N = 64$. ○, zeros; **x**, poles.

domain [2]. There are three major disadvantages of this procedure, as further verified in the numerical simulations and the experimental results of Sections 4 and 5:

(A) An accurate modal identification of the structure is needed, in order to exhibit all the modes contributing to the response.

(B) According to the proposed procedure [2], in case that the initial impulse sequence must be extended in order to cover one additional natural frequency of the structure, a further convolution is necessary with an additional single-mode shaper around this specific natural frequency. As an unavoidable result, the final input shaping sequence is further delayed in time.

(C) Due to the convolution procedure, lobes exist in the frequency response function (“sensitivity curve”) of the input shaping sequence. Since the value of these lobes may exceed the maximum permissible residual vibration error over extended frequency regions contrarily to Requirement (R.d) in Section 3.2, the actual robustness offered by input shapers may not cover natural frequencies which might have not been identified by the modal analysis procedure, or natural frequencies with significantly time varying characteristics.

Contrarily, in the design process of [16] the robustness (stop-band region of the filter) is increased in a structured and systematic way by adding more equidistant filter pulses, while simultaneously selecting the pulse repetition period T_S in an optimal way, which avoids as much as possible the further unnecessary increase of the delay introduced by the filter. This fact can be observed in Fig. 2, where the relative filter robustness is increased from $r_R = 1.85$ in the case of 4 filter pulses to $r_R = 11.72$ for 16 pulses and to $r_R = 51.76$ for 64 filter pulses with a marginal increase in the relative delay introduced by the filter from $d = 1.0$ in the case of 4 pulses to $d = 1.16$ for 16 pulses and $d = 1.19$ for 64 pulses.

As further shown at the relative robustness values in Fig. 4 of Ref. [16], the robust region of the three best performing filters for a filter order above $N = 128$, can extend up to multiples of orders of 100 of the lowest expected natural mode of the system. For example, the relative robustness of a Parks–MClellan filter type of order $N = 128$ is $r_R = 105$ for a 5% residual vibration error, implying that the robust region extends up to 105 times the lowest expected natural frequency of the system.

Thus, the filter robustness can be dramatically increased by increasing the filter order N. The only practical limitation is the numerical instabilities, inherent in the filter design process. For relatively high filter orders of $N = 256$ the filters exhibit a maximally robust behavior, which is almost identical to the one theoretically expected. For example, such a filter presents a relative robustness width r_W of 99%, with a difference less than 1% from the theoretically expected maximum robustness and a relative robustness of $r_R = 210$ times the lowest expected natural frequency of the system. This implies that the robust region (stop-band) of the filter in this case occupies 99% of the entire filter band. Quite robust behavior is obtained also for significantly lower filter orders. For example, the filter in Fig. 2c offers a relative robustness width of 96.3% and the filter in Fig. 2b offers a relative robustness width of 85.4%. Moreover, the relative robustness width is practically insensitive to the residual vibration error.

As a result, robustness of such orders of magnitude is far beyond any one offered by existing input shaping preconditioning techniques and is more than satisfactory for practical applications, enabling the effective application of these filters in structures with densely packed modes, or in structures with significantly time-varying natural frequencies.

Equally important from the practical point of view, is that this maximal robustness is achieved, while simultaneously optimizing the delay time and the permissible vibration error of the filter to quite satisfactory values. For example, the Parks–McClellan filter of $N = 256$ mentioned above introduces a residual vibration error at most of 5% and presents a delay time of 1.20 times the maximum expected natural period of the system. The optimal time behavior of these symmetric FIR filters is verified among others, by the z-plane plots of the zeros of the filter, which are all located on the unit circle (Fig. 2).

A more systematic presentation of the above properties is depicted at the delay-error-order (DEO) curves in Fig. 3 of [16] and the robustness-error-delay (RED) curves in Figs. 2, 3 and 4 of Ref. [17]. The DEO curves show that the delay introduced by each filter is strongly influenced by the maximum permissible error $(e_S)_{\text{per}}$. It becomes larger when $(e_S)_{\text{per}}$ becomes small and vice versa. For very small values of the filter order N, the minimum time delays are small and they increase as N increases. Above a certain critical value of N, the minimal time delays practically converge to a constant value independent of N. This result has also a major impact. It implies that the relative filter robustness for the filters considered can be increased just by increasing the filter order N, while retaining practically the same total filter duration time and resulting in the same residual vibration error.

Similarly to the case of FIR filters, a general design procedure has been proposed in Ref. [17] also for the selection of the parameters of any IIR filter type, which optimally fulfills the requirements of Section 3.2. However, analysis of the performance of four types of conventional IIR filters [17] has shown that although this type of IIR filters may offer a number of advantages, such as reduction of computational effort, as well as

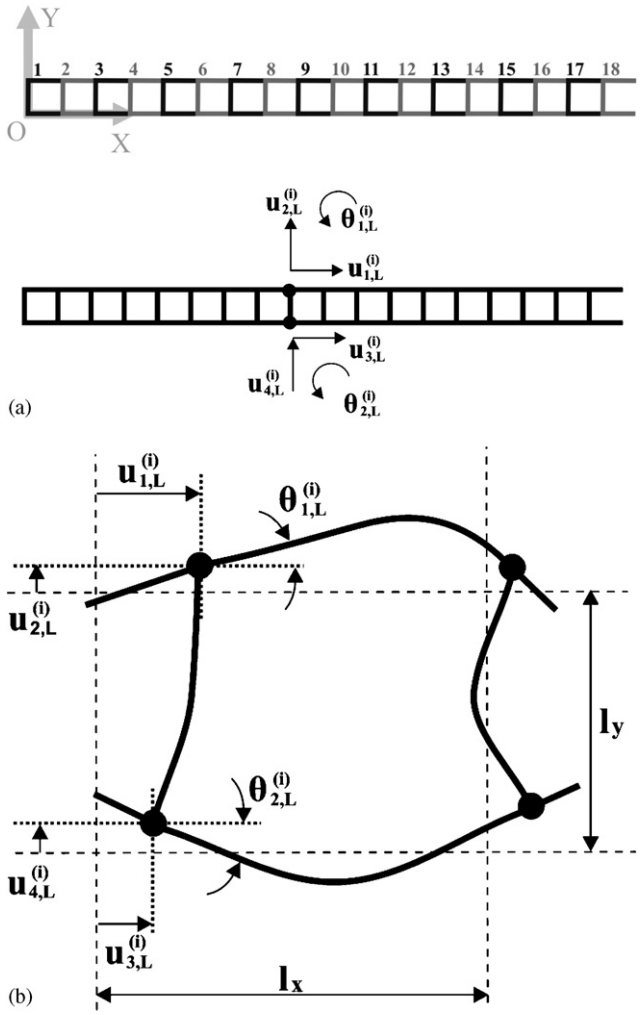

Fig. 3. Multibay truss considered in the numerical simulations: (a) the 18 periodic sets (bays) of the truss structure and (b) degrees of freedom defined at an individual truss beam.

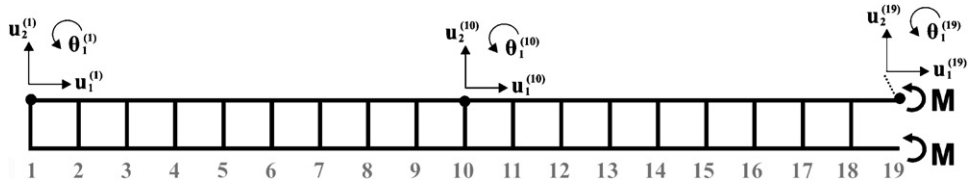

Fig. 4. Location of the excitation forces of the truss structure.

a better overall vibration suppression quality, the three best performing FIR filters in Ref. [16] present a better behavior in terms of time delay introduced, compared to the four conventional filters in Ref. [17] for equal requirements of robustness and maximum permissible vibration error.

4. Numerical simulations

4.1. Truss description

The truss structure examined (Fig. 3) is a typical flexible structure with multiple and densely spaced modes, already analyzed in Ref. [21]. It consists of 18 periodic sets (bays) connected by clamped joints. Each periodic set consists of coupled beams undergoing axial and bending vibrations. The joints connecting the beams of each periodic set transmit longitudinal (axial) and transverse forces, as well as bending moments.

The (6×1) vector $u_L^{(i)}$ of the degrees of freedom at the left boundary of the ith periodic set can be defined as follows:

$$u_L^{(i)} = \left[u_{1,L}^{(i)} \quad u_{2,L}^{(i)} \quad \theta_{1,L}^{(i)} \quad u_{3,L}^{(i)} \quad u_{4,L}^{(i)} \quad \theta_{2,L}^{(i)} \right]^{\mathrm{T}}, \tag{15}$$

where $u_{p,L}^{(i)}$ and $\theta_{k,L}^{(i)}$, $p = 1{-}4$, $k = 1, 2$ represent the horizontal or vertical displacements, and the rotations respectively, of the joints at the left boundary of the set (Fig. 3). In order that the truss is able to move, the truss structure is considered to be free (unsupported) in space. The conservative assumption of zero damping is considered, since damping has always a positive effect for vibration suppression. The truss is assumed to move horizontally (XY plane), in order to isolate the effects of the gravity from the effects of the motion commands.

The material properties and geometric parameters of the truss elements are:

$EI = 5.587\,\mathrm{Pa\,m^2}$ (E: modulus of elasticity, I: moment of inertia of a beam member),
$EA = 2.216 \times 10^6\,\mathrm{Pa}$ (E: modulus of elasticity, A: cross-section of a beam member),$\bar{m} = 0.0855\,\mathrm{kg/m}$ (mass per unit length of a beam member),
$\rho = 2700\,\mathrm{kg/m^3}$ (aluminium density),
$l_y = l_{\mathrm{vert}} = 0.903\,\mathrm{m}$ (length of a vertical beam member), and
$l_x = l_{\mathrm{horiz}} = 0.903\,\mathrm{m}$ (length of a horizontal beam member).

4.2. Original rigid body motion profiles

A pair of equal moments is applied to the right boundary joints of the truss, as indicated in Fig. 4. The time profile of both moments, indicated in Fig. 10(a) corresponds to the classical time optimal point-to-point motion commands, used in the case of rigid bodies. It consists first from a constant acceleration phase, with duration of 5 s under a maximum moment of 1.0 Nm, a constant velocity phase with duration of 15 s and a constant deceleration phase with duration of 5 s under a reverse maximum moment of −1.0 Nm.

Then, the system response is numerically calculated in the time domain. The corresponding spectra of the accelerations of the three degrees of freedom (horizontal/vertical displacement and rotation) for three joints of the truss (beginning/middle/end) are presented in Fig. 5. As it can be observed, although the motion profiles are properly designed for the case of a rigid body, in the case of the flexible truss they introduce a significant amount of vibrations.

We note that resonances in this system occur in dense clusters, which correspond to propagation zones of the various wavemodes of the corresponding truss of infinite spatial extent [22]. These dense clusters of eigenfrequencies are extended in a very wide frequency band (0–70 Hz). The results of this analysis coincide to the ones in the literature [19–21] and are further verified, by comparing the frequencies appearing in the spectra (Fig. 6) to the results of a parallel modal analysis, with partial results presented in Table 1.

4.3. Input preconditioning procedures

In order to suppress the excited vibrations, first a FIR filter based input preconditioning method is used. Alternatively, an IIR filter, and a specially designed input shaper are also used for comparison purposes.

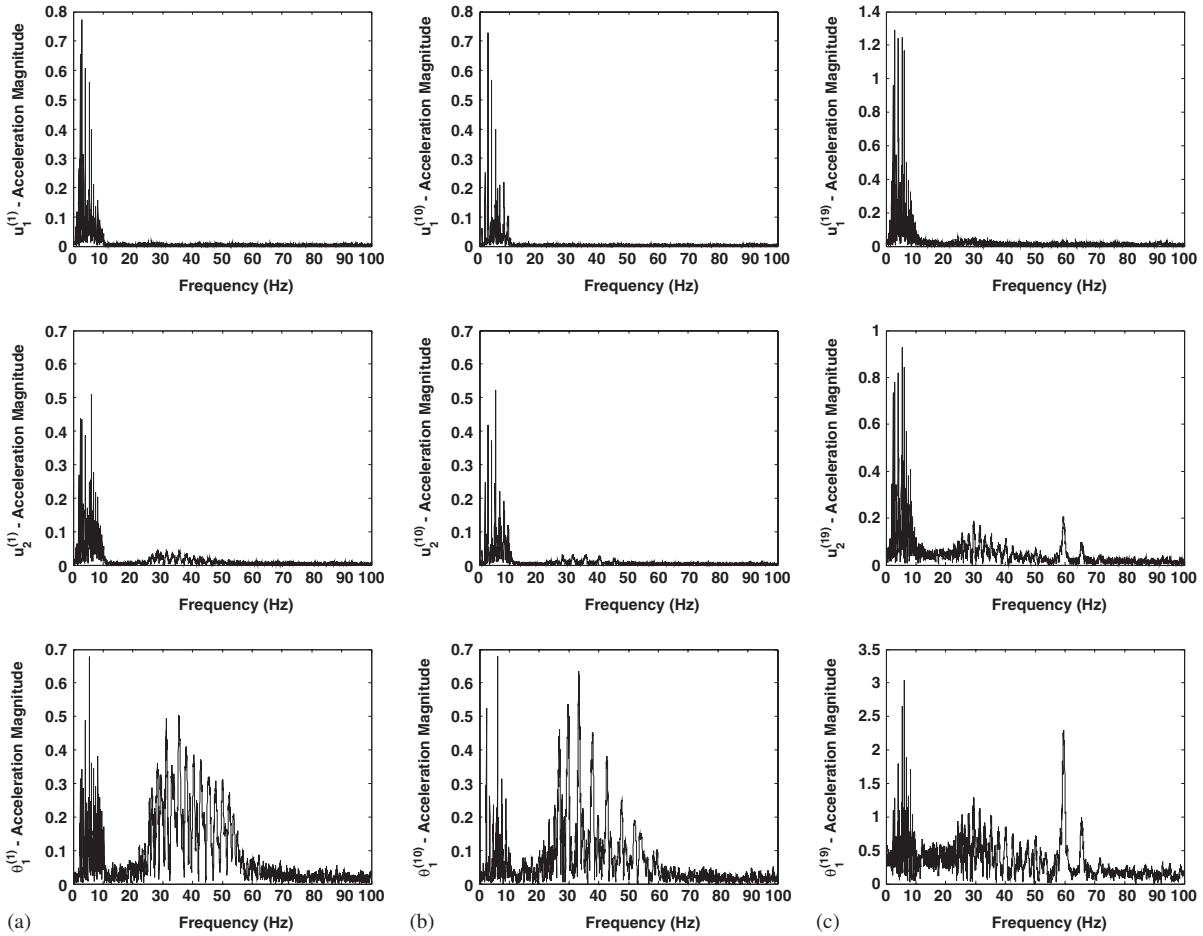

Fig. 5. Spectra of the accelerations for the three degrees of freedom (horizontal/vertical displacement and rotation), at three individual joints on the upper part of the truss: (a) joint 1, (b) joint 10 and (c) joint 19, in the case of rigid body motion pattern (Section 4.2).

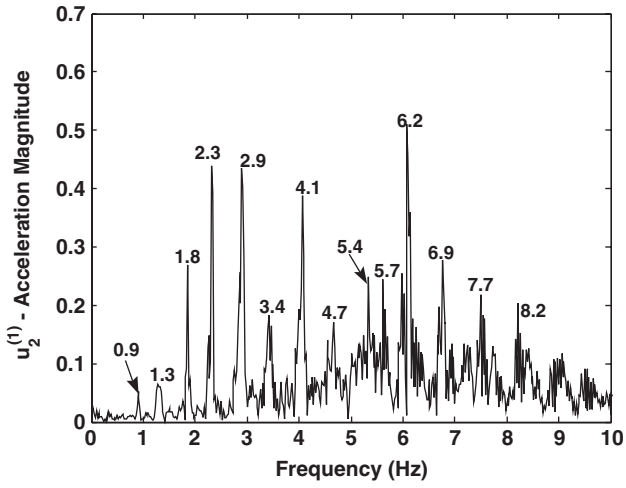

Fig. 6. Magnified view of the frequency band 0–10 Hz of the acceleration spectrum for the vertical degree of freedom at joint 1.

Table 1
The 15 first eigenfrequencies of the truss system of Section 4 as calculated via numerical modal analysis

Index	Frequency (Hz)
1	0.9083
2	1.3102
3	1.8720
4	2.3387
5	2.9316
6	3.4648
7	4.1162
8	4.1994
9	4.7185
10	5.4269
11	5.7256
12	6.2338
13	6.9630
14	7.7385
15	8.5221

4.3.1. *FIR filter design procedure*

The only basic requirement needed from the identification of the dynamic system for the application of the FIR filter, is an estimate of the lowest expected natural frequency of the system, which, according to Fig. 6, is around 0.9 Hz. The cut-off frequency of the filter is selected equal to this value.

A FIR filter, designed according to the Parks–McClellan method, is then selected. Although several types of filters can be equivalently used, FIR filters of the Parks–McClellan type have been shown [16] to belong in the class of the best performing filters.

Then, the implementation of the FIR filter results quite easily from the straightforward and systematic procedure, described in Ref. [16]. The permissible vibration error is set to 5%. The stop-band of the filter should cover a region between 0.9 and 70 Hz, which results in a relative robustness or approximately $r_R = 78$. From Fig. 4 in Ref. [16] it is concluded that a filter with an order on $N = 96$ would be in principle satisfactory for the application. However, since the delay introduced by a filter of this order is practically the same if the filter order is further increased according to Fig. 3 in Ref. [16], the filter order is finally selected to be $N = 256$, in order to present an almost maximally robust behavior, with a relative robustness of almost 99%.

According to Fig. 3 in Ref. [16], the relative delay introduced by the filter results in approximately 1.2 times the highest natural period of the system, which leads to a total time delay of the filtering process equal to approximately 1.32 s.

The rest of the filter design parameters are retrieved from the DEO curves and the look-up tables corresponding to the specific filter [16]. The filter transfer function is shown in Fig. 7(a). The stop band of the filter covers frequencies from 0.9 Hz up to approximately 194 Hz. It is obvious that this stop band is significantly wider than that actually needed, however no penalty is paid in terms of time delay. In Fig. 7(b) the zero-pole plot of the filter frequency function is shown. Since the zeros of the filter are uniformly distributed on the unit circle, the time optimal behavior of this filter is verified.

4.3.2. *IIR filter design procedure*

According to the design procedures in Ref. [17], a quite similar procedure to the one described in Section 4.3.1, can be followed also for the case of the IIR filter. Again, the cut-off frequency of the filter is selected equal to 0.9 Hz.

From the robustness-error-delay (RED) curves in Fig. 2 of Ref. [17], it is concluded that no conventional IIR filter from the ones considered in Ref. [17] can reach a relative robustness of $r_R = 78$ required for the application, without introducing a far more significant delay than that introduced by the FIR filter. Thus, an IIR filter, designed according to the Chebyshev Type II method, is used. As shown in Ref. [17], among the

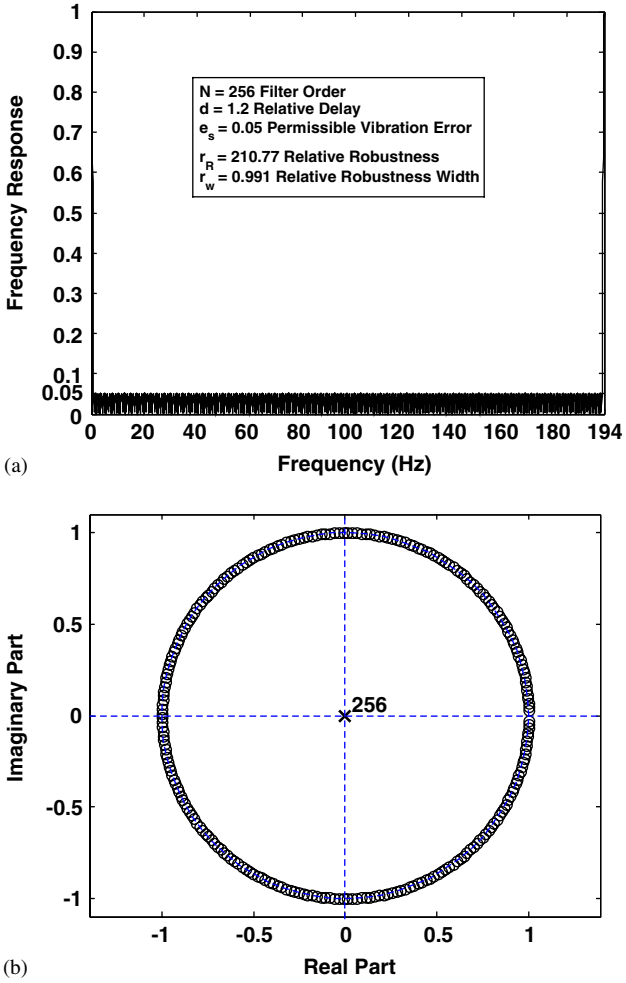

Fig. 7. (a) Frequency Response Function and (b) z-plane zero-pole plot, of the Parks–McClellan FIR filter type, used for motion preconditioning of the truss in Fig. 3. ○, zeros; **x**, poles.

other IIR filters considered, the Chebyshev Type II filters combine both robustness maximization characteristics and acceptable time delay introduction.

Then, the implementation of the IIR filter results from the procedure described in Ref. [17]. The permissible vibration error is set to 5%. From the RED curves and the corresponding look-up tables of [17], it is concluded that the minimum values of the relative delay are obtained, if the filter order is respectively selected to be $N = 4$. According to Ref. [17], the chosen filter order results in a large relative robustness of almost $r_R = 100$. The duration of the filter is 0.05 s, the total time delay introduced by the filtering process is equal to approximately 2.2 s, which is about 2 times the highest natural period, and the corresponding sampling frequency is 80 Hz.

The FRF of the IIR filter is shown in Fig. 8(a). The stop band of the filter covers frequencies from 0.9 Hz up to approximately almost 80 Hz. This stop band is slightly wider than that actually needed, in view of the actual bands of the spectra presented in Fig. 5. Nevertheless, compared to the corresponding FRF of the FIR filter, as depicted in Fig. 7(a), this filter presents a much more smooth frequency response, almost zero in an extended region of the frequency plane, indicating greater efficiency in terms of vibration reduction. The zero-pole plot of the IIR filter frequency function is shown in Fig. 8(b). The zeros of the system lie also on the unit circle, close to the zero of the imaginary axis.

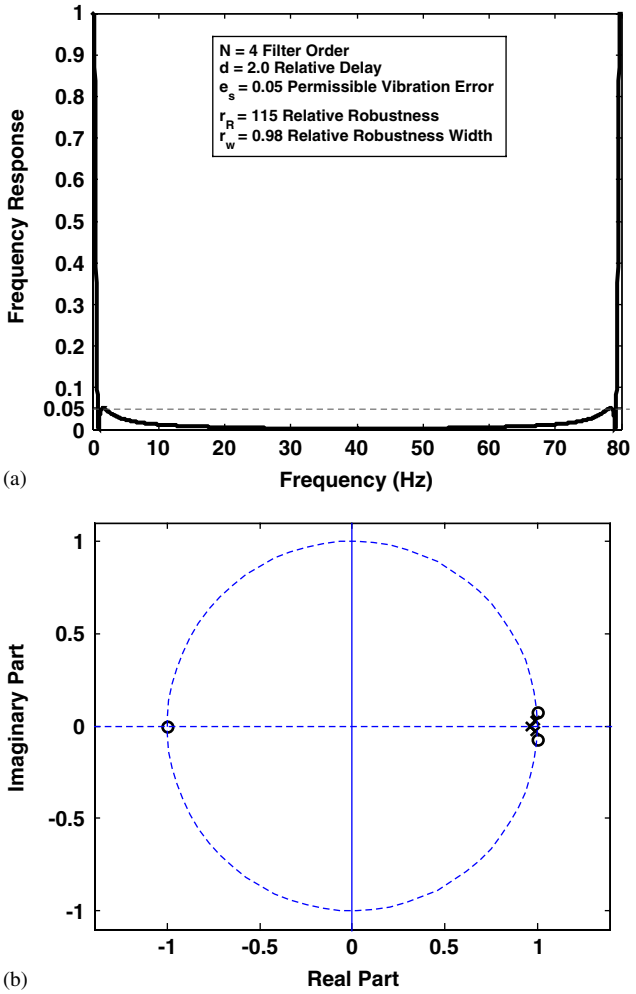

Fig. 8. (a) Frequency Response Function and (b) z-plane zero-pole plot, of the IIR Chebyshev Type II filter type, used for motion preconditioning of the truss in Fig. 3. ○, zeros; **x**, poles.

4.3.3. Input shaper design procedure

Input shaping is basically focused to design shapers able to suppress vibrations in local areas around specific and discrete natural frequencies of the system. Thus, the typical procedure to design an input shaper would first require an extensive modal identification procedure for the structure. In view of the spectra in Fig. 5, this results in being a rather cumbersome task with doubtful results. However, for performance comparison purposes, the design of an input shaper is also attempted, according to the following three basic design criteria, set accordingly to the two previous filter cases:

1. The cut-off frequency of the input shaping sequence should coincide with the lowest natural frequency of the dynamic system (0.9 Hz).
2. The total time delay of the input shaper should not exceed the time delay induced by the FIR filter.
3. The stop-band of the sensitivity curve should preserve a maximum stop-band ripple of 5%, covering as much frequency range as possible, away from the cut-off frequency.

A large variety of input shapers can be in principle chosen. However, due to the robustness requirements of the application, a convolution of two single-mode Extra Insensitive shapers together is selected. Based on the three criteria set, the input shaper has been developed following the approach of [2] by convolving two

2-Hump EI shapers, designed for dynamic systems with undamped modes at 1.42 and 5.4 Hz, respectively. The frequencies of 1.42 and 5.4 Hz correspond respectively to the beginning and to the middle of the main excited frequency band (0.9–10 Hz, Fig. 6). The hybrid input shaper imposes a time delay of 1.32 s, equal to the delay induced by the application of the FIR filter.

The sensitivity curve of the input shaper is shown in Fig. 9, in comparison to the frequency transfer function of the FIR filter. The input shaper is covering a frequency band starting from the lowest natural frequency until 2 Hz, and several other frequency bands in small extended regions of the frequency plane (3.2–7.8 Hz, 9.5–10.5 Hz, etc.) However, it is easily observed that although the extra insensitive family of input shapers has been chosen and further convolved, it fails to cover satisfactory the stop-band requirements of the application. This can be only achieved by a number of further convolutions using additional natural frequencies in the band, which leads to more delay than that of the FIR filter and to a more complicated design process.

4.4. *Effects of the preconditioned inputs*

The three approaches of Section 4.3 are then used to precondition the commanded inputs of Section 4.2. The resulting inputs are shown in Fig. 10, in comparison to the original time-optimal inputs.

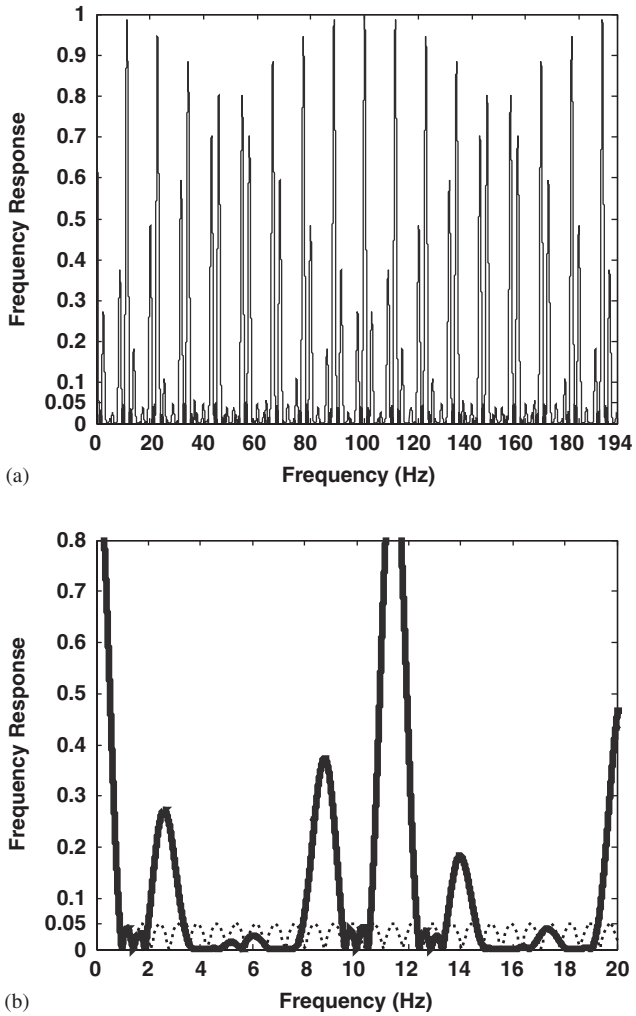

Fig. 9. (a) Sensitivity curve (FRF) of a hybrid input shaper, used for input preconditioning of the truss in Fig. 3, (b) magnified view of Fig. 9(a) vs. FRF of the FIR filter of Fig. 7. ——, input shaper; -----, FIR filter.

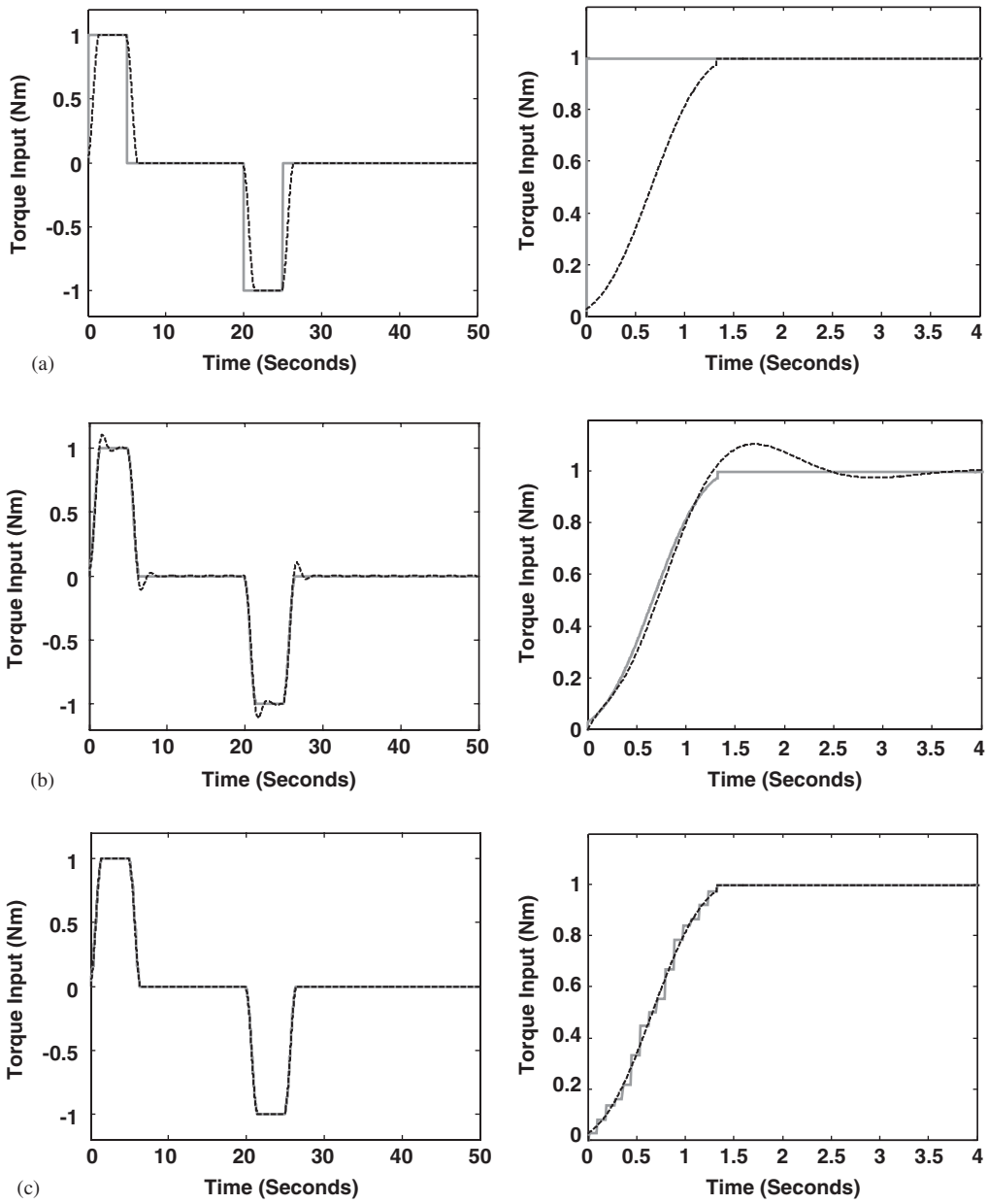

Fig. 10. (a) Profiles of the time-optimal compared to FIR filtered commanded inputs ——, time optimal; – – – –, FIR filter, (b) profiles of the FIR filtered compared to IIR filtered commanded inputs ——, FIR filter; – – – –, IIR Filter and (c) profiles of the input shaped compared to FIR filtered commanded inputs ——, input shaper; – – – –, FIR filter, and magnified views in the period from 0 to 4 s.

The resulting acceleration time series for horizontal and vertical directions, and rotations, at two individual joints of the truss are illustrated in Fig. 11 for the FIR filter, together with the original vibrations. It can be easily observed, that the fluctuations and the magnitudes of the vibration are dramatically diminished, both during the transient and the residual states of the motion. Then the corresponding results for the cases of the IIR filter and of the hybrid input shaper commanded inputs, are separately compared to the results of the FIR filter, in Figs. 12 and 13 accordingly.

With respect to the vibration minimization target, it is easily noticed that both FIR and IIR filtered inputs are substantially more effective, compared to the input shaper results. From this point of view, the most outstanding result is achieved by the application of the IIR preconditioned command, since the resulting

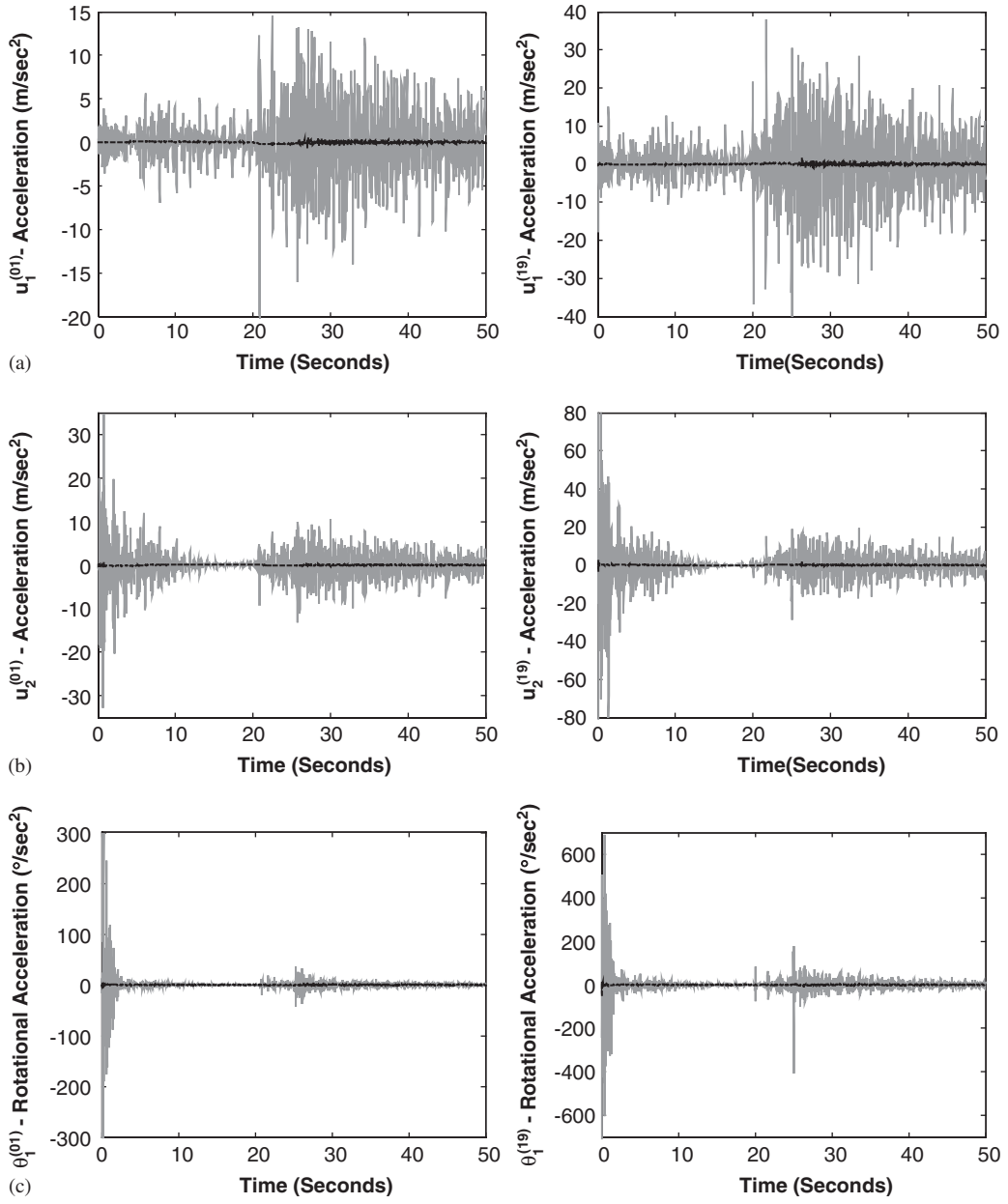

Fig. 11. Acceleration time series for (a) horizontal direction, (b) vertical direction and (c) rotation, at two individual joints of the truss (1, 19), for time-optimal and FIR filtered command inputs. ——, time optimal inputs; - - - - -, FIR filter inputs.

vibration amplitudes remain practically negligible both during the transient, as well as the residual response. Contrarily, the FIR preconditioned command may not provide the almost perfect vibration suppression capability of the IIR filter, but it introduces 40% less time delay. Additionally, in view of its FRF in Fig. 7, it is readily imposed that it renders the dynamic system almost immune to any change of the operating conditions. This is justified by the very large robustness that extends to 194 Hz, which is almost 2.5 times the robustness provided by the IIR filtered command.

Further details on the performance of all three methods can be revealed in Figs. 14–16, where the spectra of the corresponding accelerations are presented. Since the FRF of the IIR filter in Fig. 8 presents a uniform and almost equal to zero curve, it attenuates more effectively the vibrations in most part of the stop-band. The

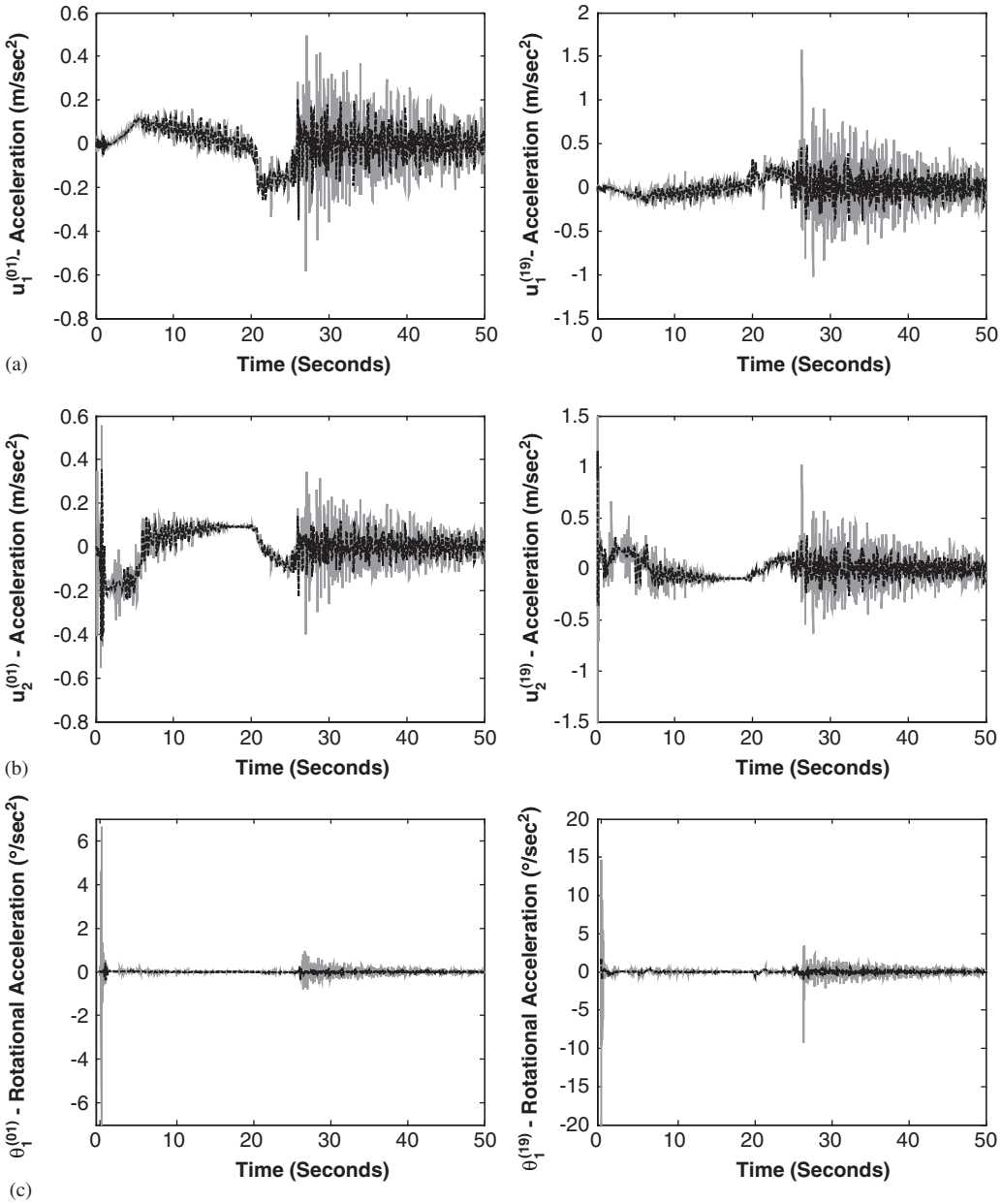

Fig. 12. Acceleration time series for (a) horizontal direction, (b) vertical direction and (c) rotation, at two individual joints of the truss (1, 19), for FIR and IIR filtered command inputs. ——, FIR filter inputs; - - - - -, IIR filter inputs.

FRF of the FIR filter in Fig. 7 presents characteristic lobes, inherent in all FIR filter types, and thus it prevents the perfect elimination of the vibrations. However, these lobes form a uniform periodic structure with a maximum value of ripples equal to 5%, which enables the fulfilment of the residual vibration error criterion. Contrarily, a large number of lobes of the FRF of the input shaper in Fig. 9 exceed the value of 5%, which prohibits the elimination of vibrations in extended regions of the stop-band.

In view of Figs. 11, 12 and 13 further aspects of the operation of the filters are revealed. The traditional practice of "instantly" applying all the available power of the system in the form of a "bang-bang" motion type, although theoretically time minimal, produces vibrations, which in turn either require further power consumption in order to be diminished or, in the present case, result in unpredictable motion. Contrarily the

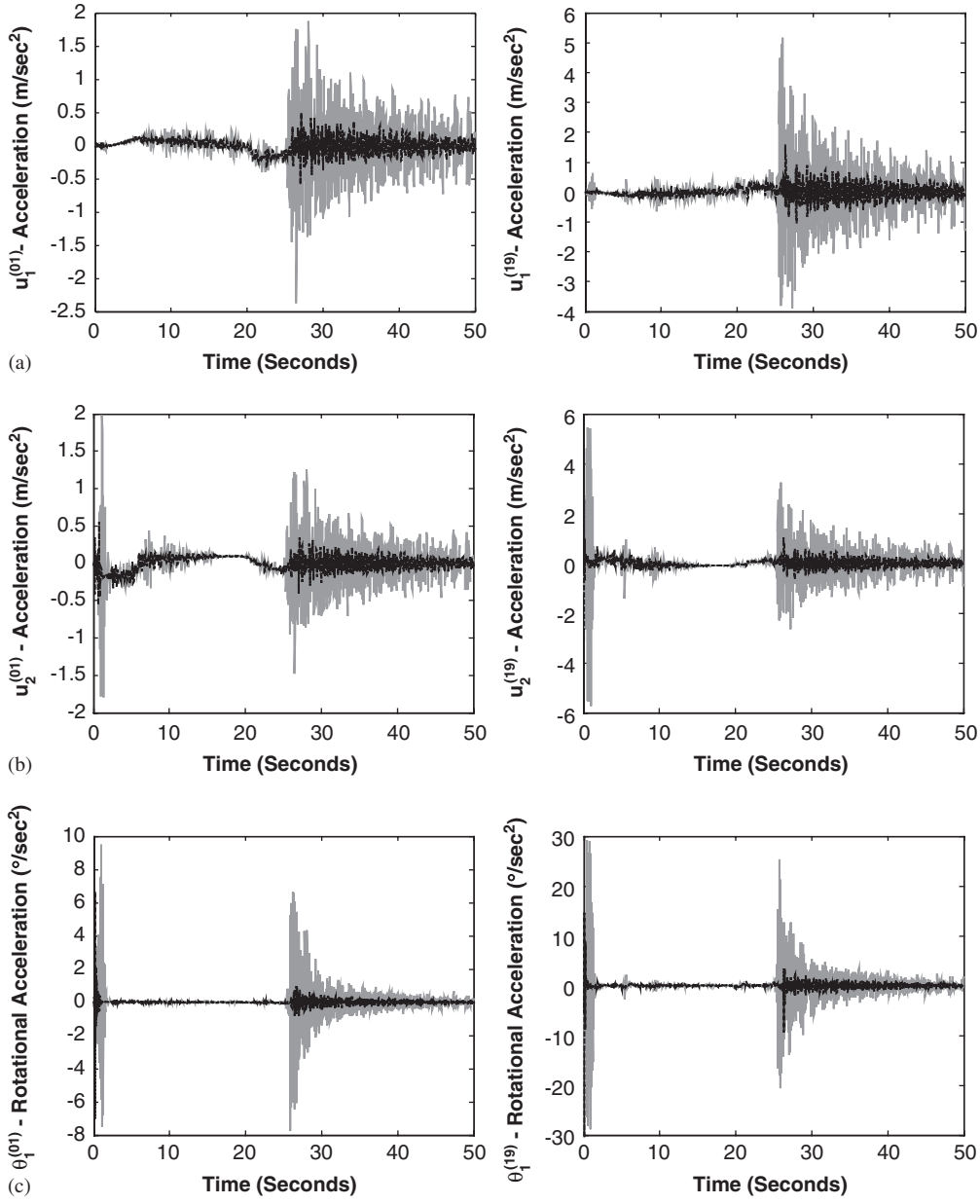

Fig. 13. Acceleration time series for (a) horizontal direction, (b) vertical direction and (c) rotation, at two individual joints of the truss (1, 19), for FIR filtered and input shaper convolved command inputs. ——, input shaper inputs; - - - - -, FIR filter inputs.

application of the filter results in an optimally distributed power supply to the system, preventing the generation of vibrations from the beginning of the motion.

5. Experimental results

5.1. Brief description of the experimental setup

Experiments were conducted for the motion command preconditioning of an aluminum truss. As shown in Fig. 17, the truss is fixed at the end point of the vertical arm of a 3-degrees-of-freedom spatial hydraulic

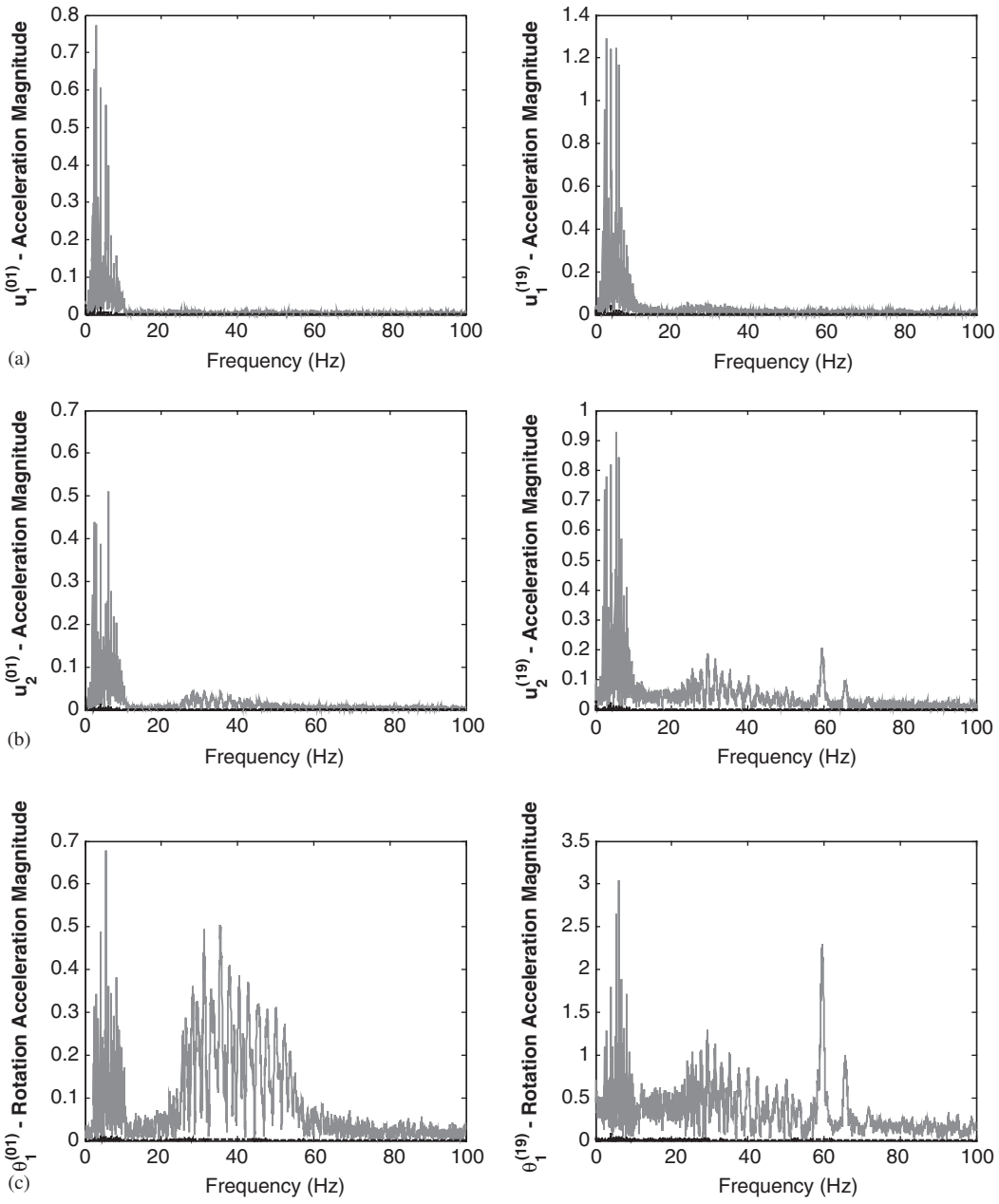

Fig. 14. Spectra of the accelerations for (a) horizontal direction, (b) vertical direction and (c) rotations, at two individual joints of the truss (1, 19) for time-optimal and FIR filtered command inputs. ——, time optimal inputs; - - - - -, FIR filter inputs.

manipulator. The hydraulic manipulator used is of Cartesian type, constructed by three independent linear axes of motion, perpendicular to each other (Fig. 17). A schematic of the subsystems of the manipulator can be seen in Fig. 18 for the case of axis-1. Each axis uses a hydraulic radial piston motor. Rotational motion is converted to linear one through a toothed ruler. All axes are completely identical in construction, but they have highly different moving masses (i.e. 350 kg for the first axis, 120 kg for the second, and 20 kg for the third).

5.1.1. Truss description

The experimental flexible structure is designed to include a number of attributes associated to large flexible structures, and especially to their characteristics related to the excitation of lightly dumped and, foremost,

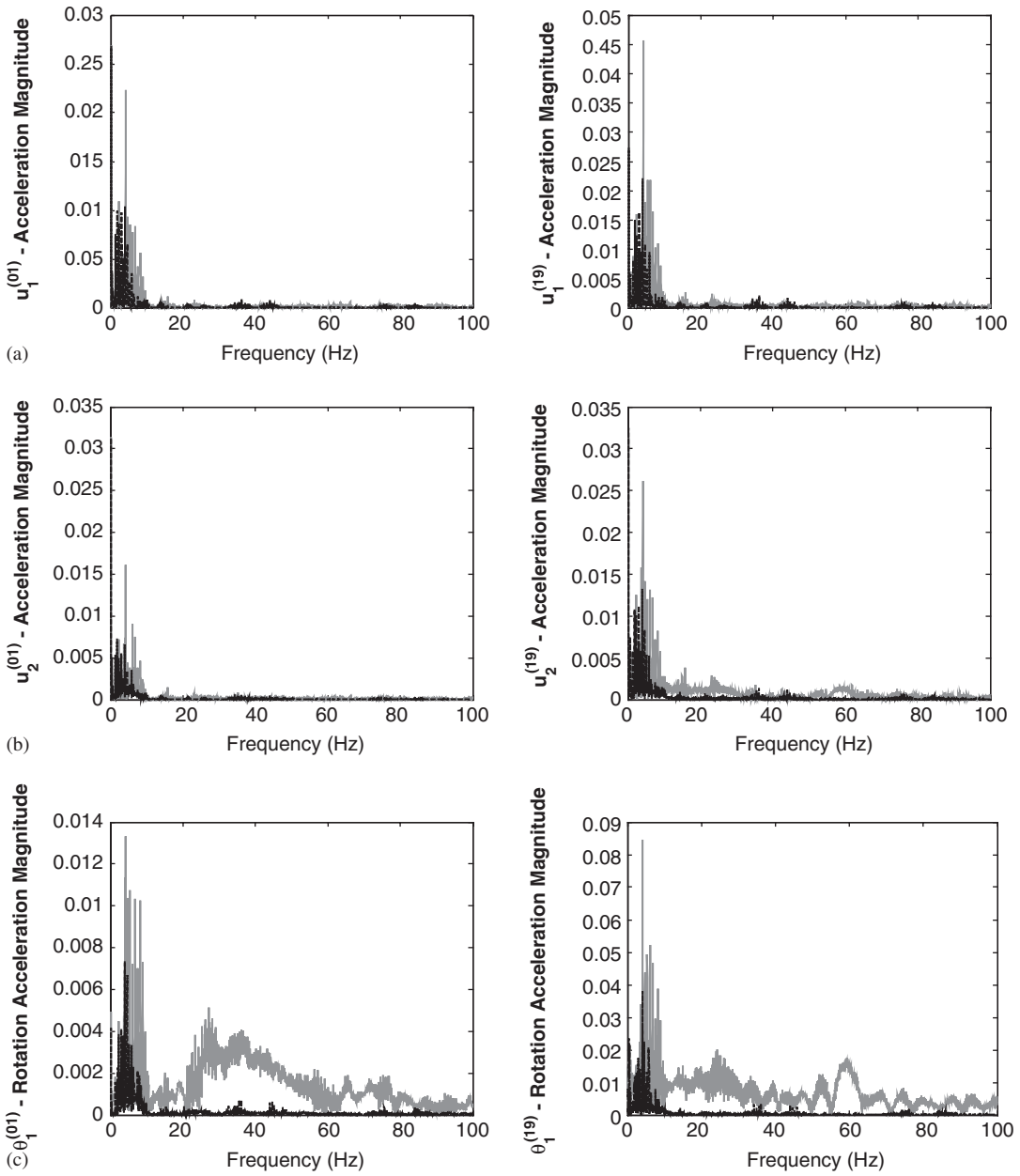

Fig. 15. Spectra of the accelerations for (a) horizontal direction, (b) vertical direction and (c) rotation, at two individual joints of the truss (1, 19), for FIR and IIR filtered command inputs. ——, FIR filter inputs; - - - - -, IIR filter inputs.

closely spaced modes. In addition to these considerations, expandability of the structure has been taken into account, following a modular construction approach, which also provides a means for increasing the modal density in a frequency range of interest.

The structure examined (Fig. 19a) is an aluminum-made truss consisting of 2 sets (bays) connected by properly designed clamped joints (orthogonal mating fixtures and two bolts). The first bay is 0.5 m long and 0.5 m wide, while the second bay is 1.0 m long and 0.5 m wide (Fig. 19b).

The assembled truss is fixed at a rigid iron-made mounting, which in turn is properly attached at the end point of the vertical arm (axis-3) of the manipulator. The entire structure is positioned parallel to the horizontal plane. In order to alleviate the problem of buckling of the longerons due to the excitation of

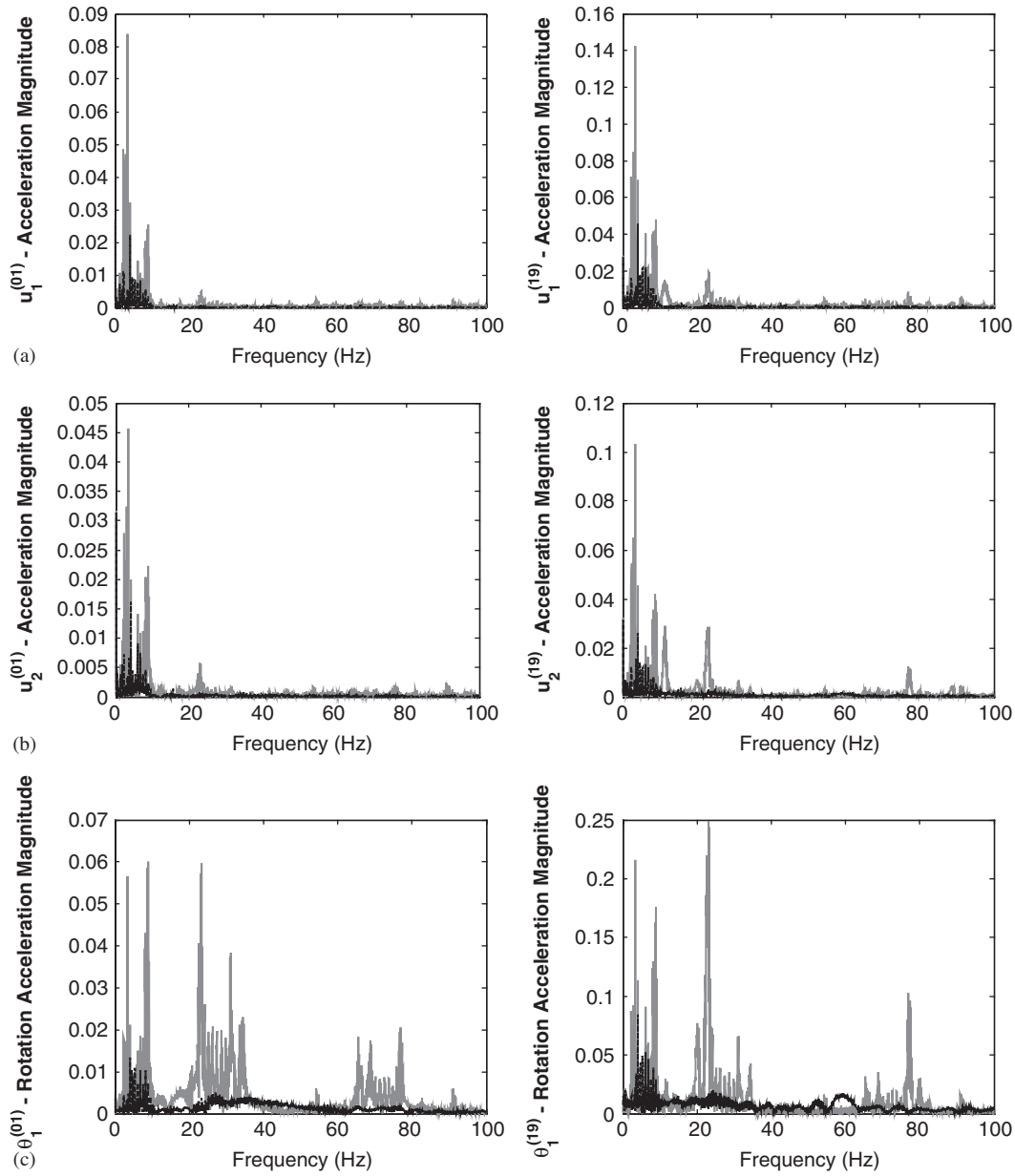

Fig. 16. Spectra of the accelerations for (a) horizontal direction, (b) vertical direction and (c) rotation, at two individual joints of the truss (1, 19), for input shaper convolved and FIR filtered command inputs. ——, input shaper inputs; - - - - -, FIR filter inputs.

torsional natural frequencies during the motion and the inherent deflexion of the flexible structure due to the influence of gravity, the height of each beam was picked to be large enough, equal to 40 mm, stiffening that way the truss in the z-direction.

The truss follows a linear motion of the manipulator along the axis-2. During and after the completion of each motion, the coupled beams of each of the two sets undergo axial and bending vibrations. The joints connecting the beams transmit longitudinal (axial) and transverse forces, as well as bending moments.

The properties of the truss elements are:

$A = 4 \times 10^{-5}\,\mathrm{m}^2$ (A: cross-section of a beam member),$\bar{m} = 0.0844\,\mathrm{kg/m}$ (mass per unit length of a beam member),

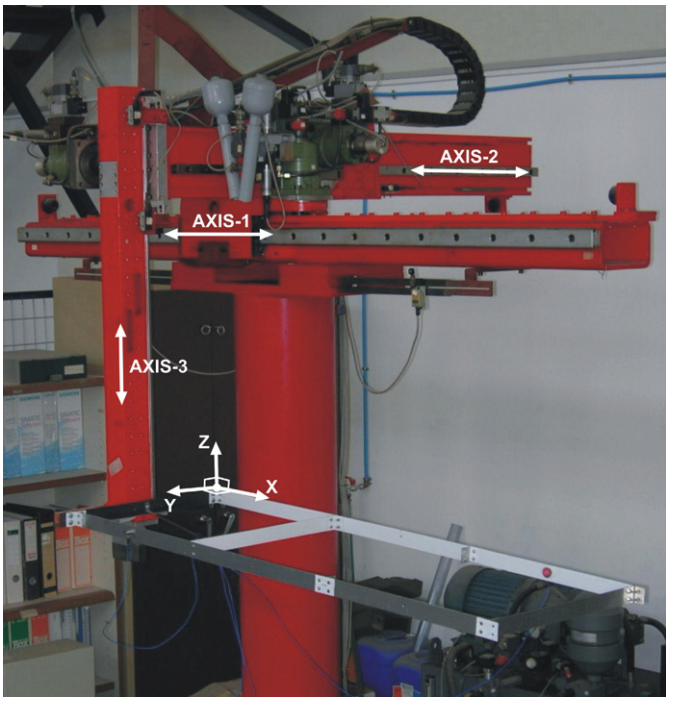

Fig. 17. View of the hydraulic manipulator with 3-degrees-of-freedom, and the flexible truss, fixed on axis-3.

$E = 2,06,800 \times 10^6$ Pa (E: modulus of elasticity) and
$\rho = 2700\,\mathrm{kg/m^3}$ (aluminium density).

5.1.2. Measurement system

The measurement system used is properly designed to accomplish simultaneously two separate tasks: (a) command signal generation, and (b) data acquisition and storage. The whole system is built on the basis of an industrial PXI-1010 chassis of National Instruments. The core of the system is the embedded controller NI PXI-8145 RT that operates in real time. A Motion Controller card (PXI-7344), and a Data Acquisition card (PXI-6040E Multifunction I/O) are mounted into slots adjacent to the controller, communicating and interacting with it through the PXI backplane local bus.

A block diagram of the experimental setup is shown in Fig. 20. The input to the system is the desired motion profile to be followed by the manipulator. The input is properly scaled in the motion controller, and the resulting voltage signal (± 10 V) is fed to the current amplifier (Rexroth VT-SR1-1X) of the servo-valve. The command signal from the drive is fed to the solenoid actuator (Rexroth Model 4 WS 2 EE 10-4X), and the corresponding reference motion is obtained. The precise position of the axis is obtained by an incremental angle encoder (Heidenhain ROD 420), which is also used for feedback of the closed-loop control system.

Two ICP accelerometers of PCB Piezotronics (Model 352C33) are used for the measurement of the excited vibrations of the truss during and after its motion, with positions shown in Fig. 19b. The accelerometers have a flat frequency response between 0.3 and 10 kHz, their sensitivity is 100 mV/g, and they provide a maximum of ± 10 V output at peak accelerations of the input disturbance. The accelerometer outputs are acquired by the data acquisition card, digitized by its 12-bit A/D converter, and stored temporarily to the RAM of the embedded controller.

5.2. Original rigid body motion profiles

A specific motion profile is applied to the second axis of the manipulator, and correspondingly to the truss. The time profile motion, indicated in Fig. 24, corresponds to a classical trapezoidal point-to-point motion

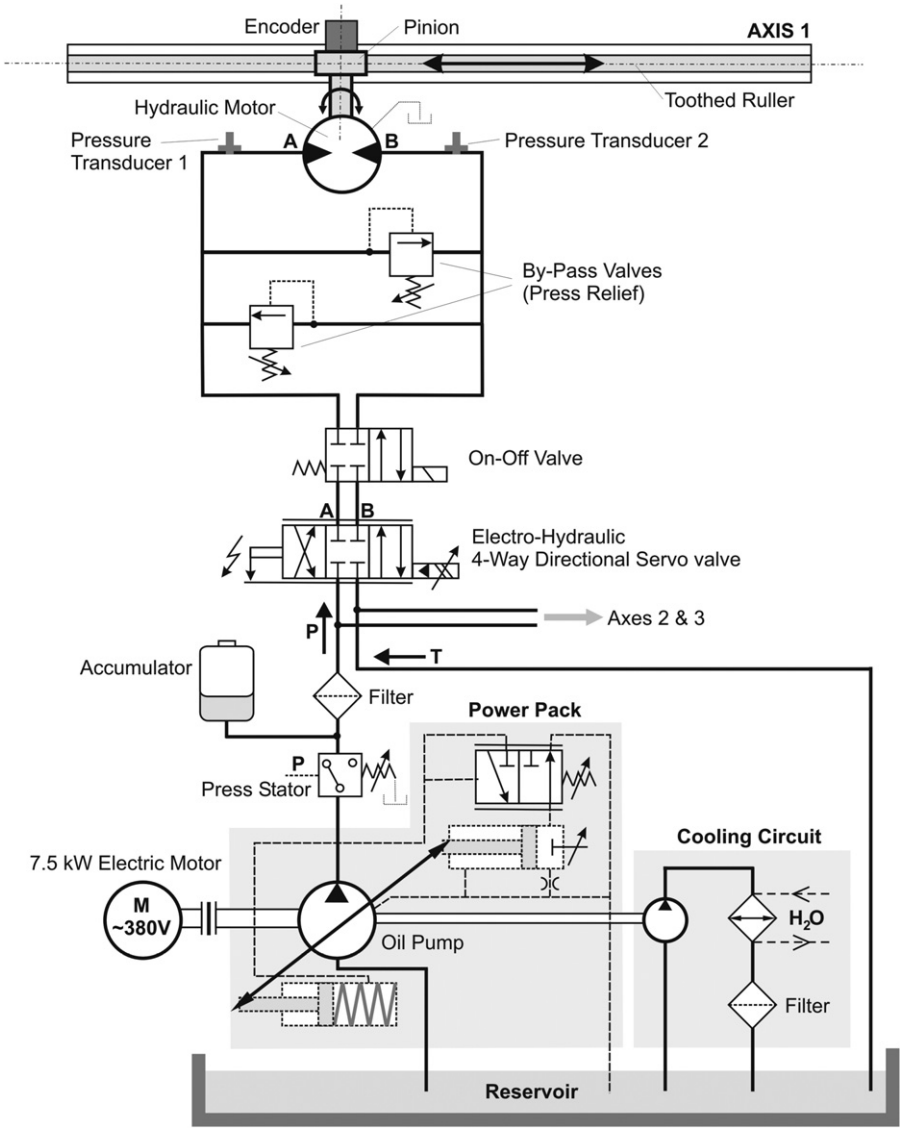

Fig. 18. Schematic of the subsystems of the hydraulic manipulator for the case of axis-1.

command, typically used in the case of rigid bodies. It consists first from a constant acceleration phase, with a duration of 0.08 s, a constant velocity phase of 0.375 m/s with a duration of 0.84 s, and a constant deceleration phase with a duration of 0.08 s.

The corresponding acceleration spectra from the two accelerometers are presented in Fig. 21. As it can be observed, the motion profiles introduce a significant amount of vibrations. Resonances in this system occur in dense clusters extending in a very wide frequency band (0–75 Hz), in both spectra estimated. The magnified view of the acceleration spectrum for the accelerometer at position A2 (Fig. 22) shows characteristically this aspect.

5.3. Input preconditioning procedures

In order to suppress the excited vibrations, a FIR filter based input preconditioning method is implemented. For comparison purposes, a specially designed convolved input shaper is also considered.

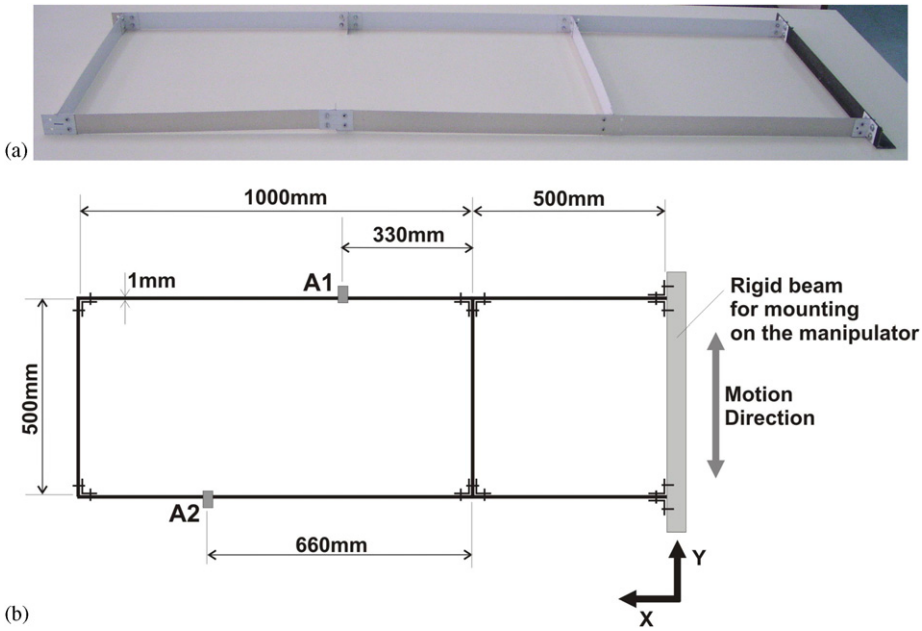

Fig. 19. (a) View of the flexible truss constructed for the experimental applications and (b) the exact measurement points for the accelerations on the flexible truss.

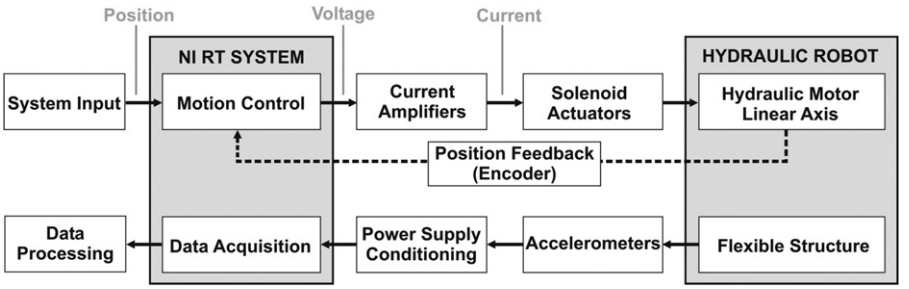

Fig. 20. Block diagram of the experimental setup.

5.3.1. FIR filter design procedure

The FIR filter is designed according to the same concepts described in Section 4.3.1. First, the cut-off frequency of the filter is set to 0.4 Hz, which according to Fig. 22 is the lowest natural frequency of the system.

The stop-band of the filter should cover a region between 0.4 and 80 Hz, which results in a relative robustness of approximately $r_R = 198$. The permissible vibration error is set to 5% and from Fig. 4 in Ref. [16] it is concluded that a filter of order $N = 240$ would be in principle satisfactory for the application. The selected filter is again of Parks–McClellan type and presents an almost maximally robust behaviour, with a relative robustness equal to 99%. The relative delay introduced by the filter results in approximately 1.2 times the highest natural period of the system, which leads to a total time delay of the filtering process equal to 3 s. The filter frequency response function is shown in Fig. 23a.

5.3.2. Input shaper design procedure

As in the case of Section 4.3.2, an accurate modal identification of the system is again a cumbersome and doubtful task, in view of the spectra of Fig. 21. Thus, the same basic remarks hold for the design of an input shaper, as in Section 4.3.2. However, the numerical results in Section 4 indicated, that the use of the FIR filter excelled in terms of vibration suppression, compared to the use of an input shaper of the same delay. Thus, in

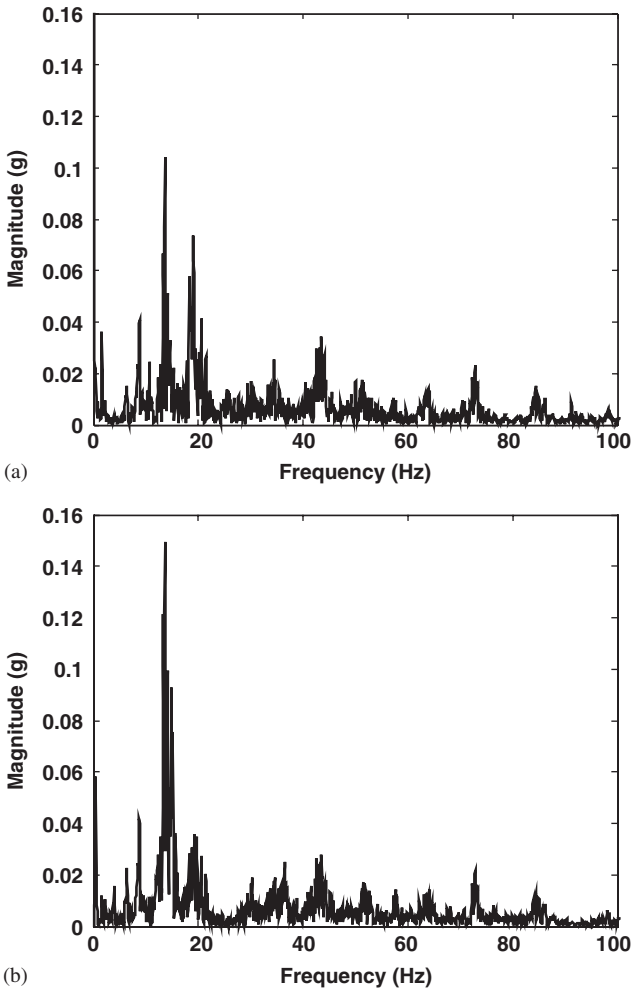

Fig. 21. Spectra of the accelerations at two individual points (A1 and A2) of the truss of Fig. 19 in the case of rigid body motion pattern.

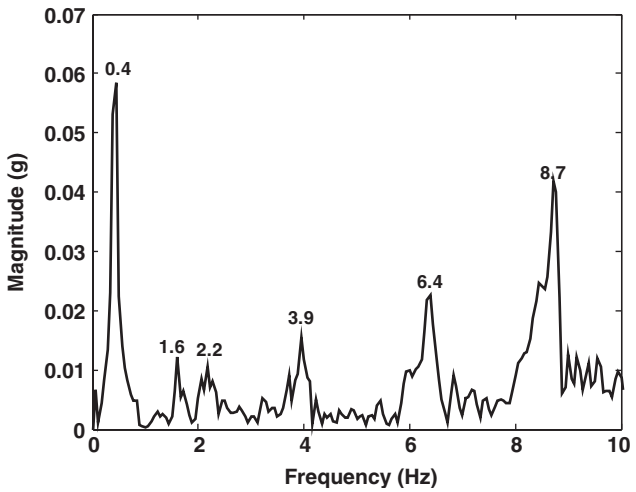

Fig. 22. Magnified view of the frequency band 0–10 Hz of the acceleration spectrum for the accelerometer at position A2.

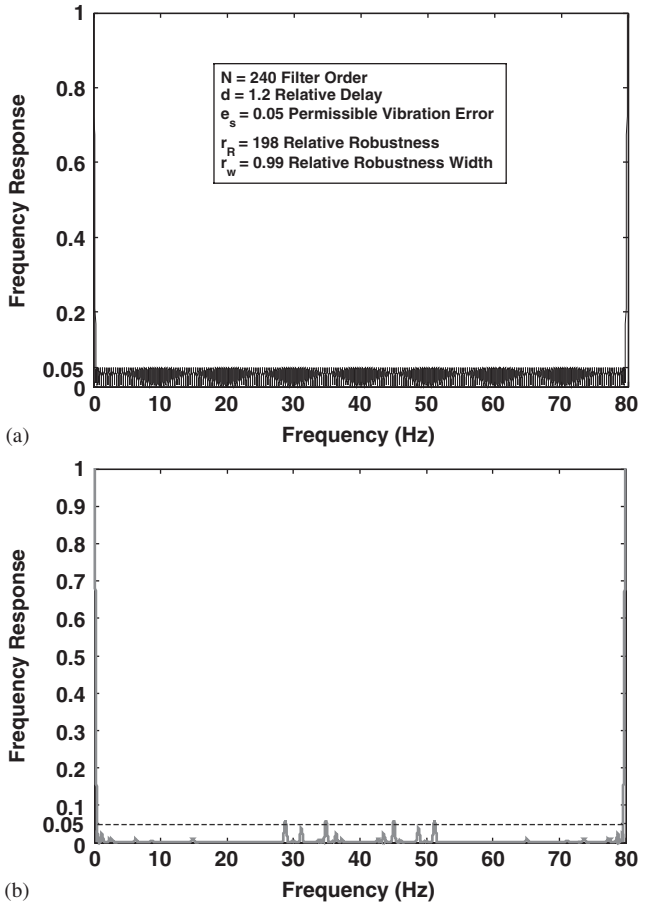

Fig. 23. Frequency response functions of (a) the Parks–McClellan FIR filter type and (b) the convolved input shaper, used for motion command preconditioning in the experimental case.

the present case a design of an input shaper with the same robustness as the FIR filter is attempted, while the criteria concerning the time delay of the input shaper are relaxed.

Therefore, the following three alternative basic design criteria are set:

1. The cut-off frequency of the input shaping sequence should coincide with the lowest natural frequency of the dynamic system (0.4 Hz).
2. The stop-band of the sensitivity curve should preserve a maximum stop-band ripple of 5%, covering the entire excited frequency band (0.4 Hz upto 75 Hz).
3. The total time delay of the input shaper should be the minimum possible.

The design logic of the convolution of single mode Extra Insensitive input shapers with 2-Humps is maintained. Initially, a 2-Hump EI shaper is chosen at 0.625 Hz, thus fulfilling the first criterion. Then four 2-Hump EI shapers are designed appropriately for dynamic systems with undamped modes at 1.45, 3.5, 7.5 and 21 Hz, and further convolved in order to cover completely the rest of the frequency region of 0.4–80 Hz. The four shapers are chosen in such a way that the corresponding suppressed frequency bands are formulated adjacently in the sensitivity curve (Fig. 4.23b).

The input shaper is covering thoroughly the frequency region of 0.4–80 Hz, while it is observed that the maximum permissible residual vibration error of 5% is consistently retained. Furthermore, it is noted that there are extended areas of the frequency plane that present a much lower stop-band ripple compared to the

level of 5%. This is due to the fact that the pattern of the sensitivity curve of a single mode input shaper repeats at all odd multiples of the mode. Thus there are areas in the frequency plane where the interaction by two or more input shapers results in lowering the acceptable vibration error.

However, the new input shaper imposes a time delay equal to the sum of the delays of each distinct input shaper, which is estimated to be 4.13 s. Compared to the time delay introduced by the filtering process, which is estimated to be 3 s, the FIR method proves to be 37% faster than the convolved input shaper with the same robustness.

5.4. Effects of the preconditioned inputs

The filter and the convolved input shaper designed in Section 5.3 are then used to precondition the commanded inputs. The resulting inputs are shown in Fig. 24, in comparison to the original rigid-body and time-optimal inputs.

The resulting acceleration time series along y-direction at the point A2 of the truss are illustrated in Fig. 25a for the FIR filtered inputs, together with the original vibrations. It can be easily observed, that the fluctuations and the magnitudes of the vibration are notably diminished, both during the transient and the residual states

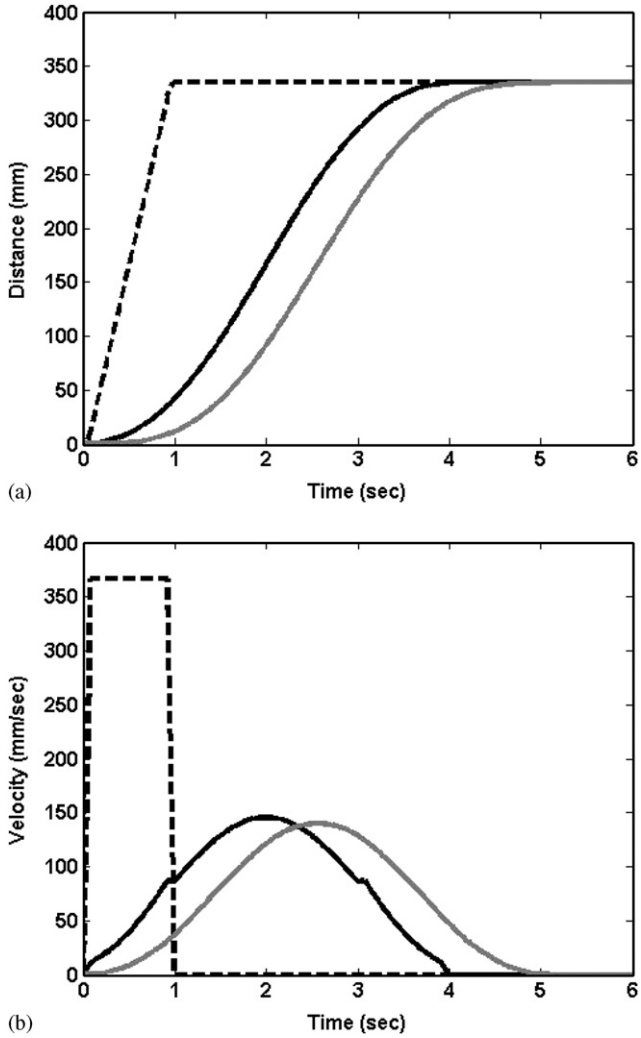

Fig. 24. Motion profiles for the experimental application: (a) displacement profiles and (b) velocity. ----, time optimal input; ——, FIR filter; ——, input shaper.

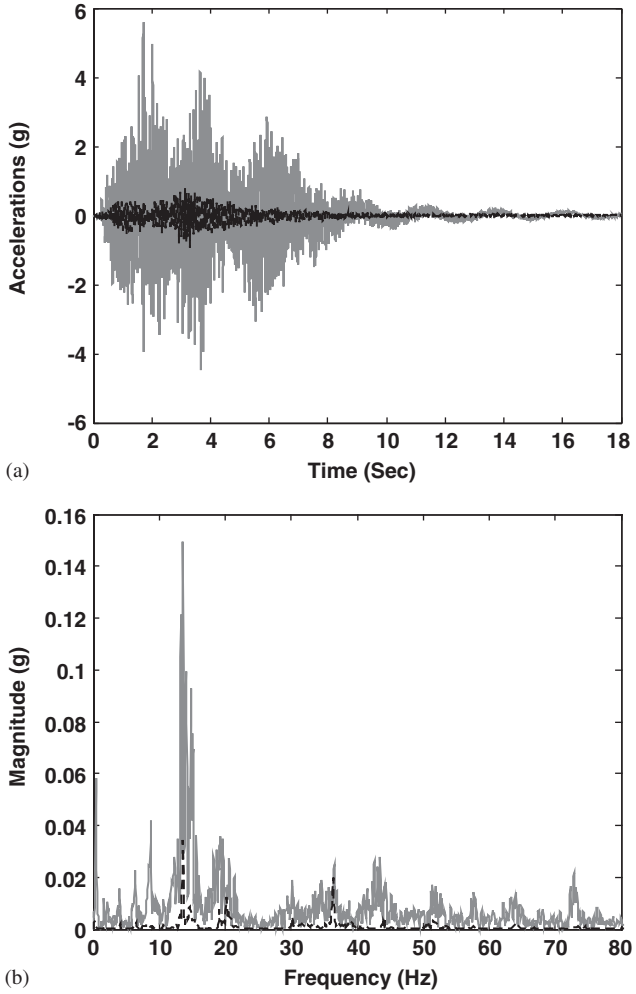

Fig. 25. (a) Acceleration time series at the point A2 and (b) the respective spectra, for the time-optimal and the FIR filtered command inputs. ——, time optimal input; - - - - -, FIR filter.

of the motion. Further details on the performance of the filtering method can be revealed in Fig. 25b, where the spectra of the corresponding accelerations are presented. The presence of characteristic lobes in the FRF of the FIR filter, as already mentioned, prevent the perfect elimination of the vibrations, while an additional source of the remaining vibrations is attributed to possible nonlinear excitations from the hydraulic circuit.

The corresponding results for the case of the convolved input shaper commanded inputs are compared to the results of the FIR filter, in Fig. 26. It is noted that the usage of the convolved input shaper results in practically the same level of remaining vibrations of the system. However, as it has already been stated, the input shaper is much slower, compared to the FIR filter.

6. Conclusion

Motion preconditioning methods can be effectively applied also for structures with multiple and densely packed modes, resulting in a drastic reduction of both transient and residual vibrations. Properly designed and implemented conventional digital filters can overcome the restrictions posed by the various existing input shaping methods for this type of structures. Due to the structured and systematic procedure by which filters of this type can be designed, they can cover uniformly the entire excited frequency band, presenting an almost

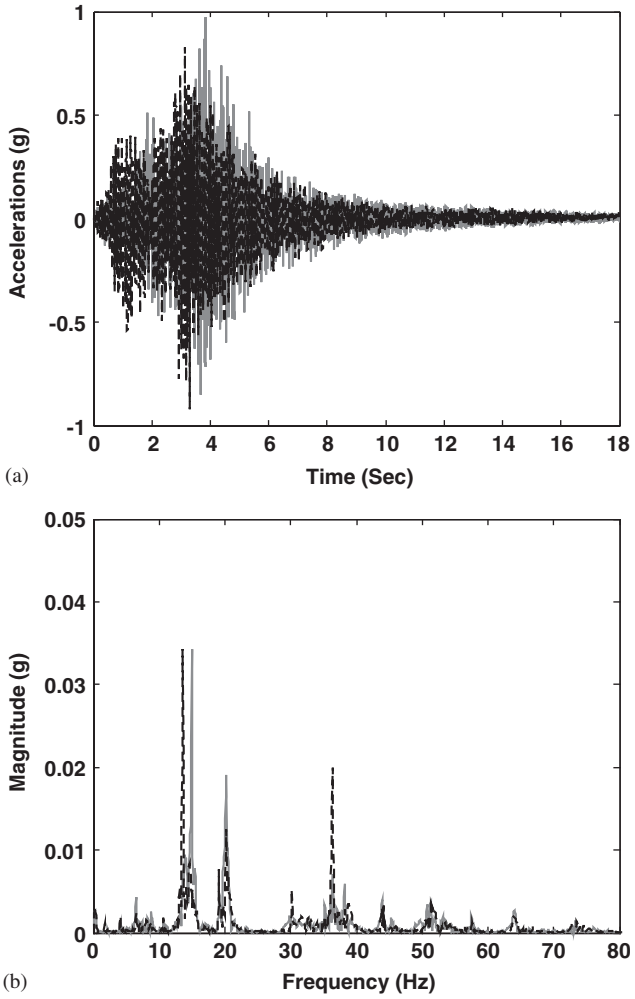

Fig. 26. (a) Acceleration time series at the point A2 and (b) the respective spectra, for the FIR filtered and the convolved input shaper command inputs. ——, FIR filter; - - - - -, input shaper.

maximally robust behavior, contrary to input shapers which are designed to cover local narrow areas around the excited natural frequencies.

As a first consequence, the implementation of digital filters is quite straightforward, requiring just an estimate of the lowest natural frequency of the system. Contrarily, input shapers require a more accurate modal identification procedure for the structure, which in the case of structures with multiple densely packed modes may result in being a rather doubtful and cumbersome task.

Among digital filters, properly designed FIR filters present a better behavior than conventional IIR filters, since they result in less time delay for the same robustness and maximum permissible vibration error. Since there does not exist currently a systematic procedure for the design of input shapers for this type of applications, attempts to design input shapers based on the existing methods result in worst performance than FIR filters, either in vibration suppression quality, or in additional motion delays.

Since the practical implementation of the method requires just the application of an already predesigned digital filter, and an estimate of the lowest expected natural frequency of the system, the method is simple to implement in actual configurations. Although, in this work, this method is presented as an open-loop control approach, it can be also efficiently combined with closed-loop control methods.

Acknowledgment

This work has been supported in part by a grant of the basic research program "Herakleitos", from the Greek Ministry of Education. The project is co-funded by the European Social Fund (75%) and National Resources (25%).

References

[1] O.J.M. Smith, *Feedback Control Systems*, McGraw-Hill, New York, 1958.
[2] N.C. Singer, W.P. Seering, Preshaping command inputs to reduce system vibration, *Journal of Dynamic Systems, Measurement and Control* 112 (1990) 76–82.
[3] W. Singhose, L. Porter, T. Tuttle, N. Singer, Vibration reduction using multi-hump input shapers, *Journal of Dynamic Systems, Measurement, and Control* 119 (1997) 320–326.
[4] J. Shan, H.-T. Liu, D. Sun, Modified input shaping for a rotating single-link flexible manipulator, *Journal of Sound and Vibration* 285 (2005) 187–207.
[5] T. Singh, S.R. Vadali, Robust time-optimal control: A frequency domain approach, *Journal of Guidance, Control and Dynamics* 17 (1994) 346–353.
[6] T. Singh, S.R. Vadali, Robust time-delay control of multi-mode systems, *International Journal of Control* 62 (1995) 1319–1339.
[7] T.D. Tuttle, W.P. Seering, Experimental verification of vibration reduction in flexible spacecraft using input shaping, *Journal of Guidance, Control, and Dynamics* 20 (1997) 658–664.
[8] U.H. Park, J.W. Lee, B.D. Lim, Y.G. Sung, Design and sensitivity analysis of an input shaping filter in the z-plane, *Journal of Sound and Vibration* 243 (2001) 157–171.
[9] L.Y. Pao, C.F. Cutforth, On frequency-domain and time-domain input shaping for multi-mode flexible structures, *Journal of Dynamic Systems, Measurement, and Control* 125 (2003) 494–497.
[10] J.M. Hyde, Multiple Mode Vibration Suppression in Controlled Flexible Systems, Master Thesis, MIT Massachusetts Institute of Technology, 1991.
[11] J.M. Hyde, W.P. Seering, Using input command pre-shaping to suppress multiple mode vibration, *IEEE International Conference on Robotics and Automation*, Sacramento, CA, 1991.
[12] B.W. Rappole, N.C. Singer, W.P. Seering, Multiple-mode impulse shaping sequences for reducing residual vibrations, in: *Machine Elements and Machine Dynamics: 23rd Biennial Mechanisms Conference*, 1994, pp. 11–16.
[13] K.W. Chang, Shaping Inputs to Reduce Vibrations in Flexible Space Structures, MSc Thesis, MIT Massachusetts Institute of Technology, 1992.
[14] M.J. Doherty, R.H. Tolson, Input shaping to reduce solar array structural vibrations, NASA/CR-1998-208698 Report, 1998.
[15] B. Murphy, I. Watanabe, Digital shaping filters for reducing machine vibration, *IEEE Transactions on Robotics and Automation* 8 (1992) 285–289.
[16] D. Economou, C. Mavroidis, I. Antoniadis, C. Lee, Maximally robust input preconditioning for residual vibration suppression using low pass FIR digital filters, *Journal of Dynamic Systems, Measurement and Control* 124 (2002) 85–97.
[17] D. Economou, C. Mavroidis, I. Antoniadis, Robust vibration suppression in flexible systems using Infinite Impulse Response Digital Filters, *Journal Of Guidance, Control, And Dynamics* 27 (2004) 107–117.
[18] D. Economou, C. Mavroidis, I. Antoniadis, Comparison of filter types used for command preconditioning in vibration suppression applications, in: *Proceedings of The American Control Conference*, Anchorage, AK, 2002.
[19] M. Xiaghong, A.F. Vakakis, Karhunen-Loeve decomposition of the transient dynamics of a multibay truss, *AIAA Journal* 37 (1999) 939–946.
[20] M. Xiaghong, A.F. Vakakis, L.A. Bergman, Karhunen-Loeve modes of a truss: transient response reconstruction and experimental verification, *AIAA Journal* 39 (2001) 687–696.
[21] E. Emaci, M.A.F. Azeez, A.F. Vakakis, Dynamics of trusses: numerical and experimental results, *Journal of Sound and Vibration* 214 (1998) 953–964.
[22] D.J. Mead, Wave propagation and natural modes in periodic systems: II. Multi-coupled systems with and without damping, *Journal of Sound and Vibration* 40 (1975) 19–39.